# Journal Pre-proof

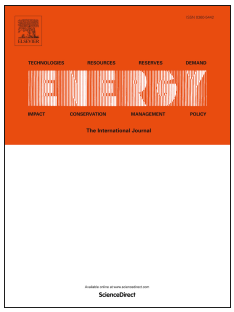

Forecasting building plug load electricity consumption employing occupant-building interaction input features and bidirectional LSTM with improved swarm intelligent algorithms

Chengyu Zhang, Liangdong Ma, Zhiwen Luo, Xing Han, Tianyi Zhao

PII: S0360-5442(23)03045-1

DOI: https://doi.org/10.1016/j.energy.2023.129651

Reference: EGY 129651

To appear in: *Energy*

Received Date: 18 April 2023

Revised Date: 25 September 2023

Accepted Date: 11 November 2023

Please cite this article as: Zhang C, Ma L, Luo Z, Han X, Zhao T, Forecasting building plug load electricity consumption employing occupant-building interaction input features and bidirectional LSTM with improved swarm intelligent algorithms, *Energy* (2023), doi: https://doi.org/10.1016/j.energy.2023.129651.

# Author statement

**Chengyu Zhang**:

Conceptualization, Methodology, Validation, Investigation, Formal analysis, Visualization, Writing-Original Draft, Writing-Review & Editing

**Liangdong Ma**:

Methodology, Data Curation, Writing-Review & Editing, Supervision

**Zhiwen Luo:**

Methodology, Writing-Review & Editing, Supervision

**Xing Han:**

Methodology, Funding acquisition, Supervision

**Tianyi Zhao:**

Conceptualization, Resources, Data Curation, Supervision, Project administration, Funding acquisition, Supervision

# Forecasting building plug load electricity consumption employing occupant-building interaction input features and bidirectional LSTM with improved swarm intelligent algorithms

Chengyu Zhang[1], Liangdong Ma[1], Zhiwen Luo[2], Xing Han[3], Tianyi Zhao[1 *]

1 Institute of Building Energy, Dalian University of Technology, Dalian, China
2 Welsh School of Architecture, Cardiff University, Cardiff, United Kingdom
3 PCI Technology Group, Guangzhou, China
* Corresponding author: zhaotianyi@dlut.edu.cn

**Abstract** Building energy consumption prediction is an essential foundation for energy supply-demand regulation. Among them, plug-load energy consumption in buildings accounts for approximately 12-50% of the total energy consumption, making plug-load energy consumption prediction crucial. However, accurately predicting plug-load electricity consumption is challenging due to the influence of random human behaviors. This study presents a comprehensive plug-load electricity consumption prediction system. First, the conventional input system based on influence factors and the novel input system based on occupant behavior probability were proposed. Second, long short-term memory (LSTM) and its improvement (Bi-LSTM) are used as the fundamental algorithm. Finally, the whale algorithm (WO), a swarm intelligent algorithm, is utilized to improve the prediction accuracy. The results show that the prediction system proposed performs better with R increased by 0.70%–23.97%, MAPE decreased by 5.33%–40.92%, and CV-RMSE decreased by 1.10%–21.08%, compared to the traditional prediction system. The combination of two input systems and four algorithms can accommodate different prediction accuracy requirements, data collection conditions, building functions, and time requirements.

**Keywords:** Building plug load, plug-load electricity consumption prediction, socket-related occupant behavior, bidirectional long short-term memory, swarm intelligent optimization

**Highlights:**

1. A novel building plug-load electricity consumption prediction system was proposed.
2. The definition and classification of building plug loads were proposed.
3. The enhanced input system based on occupant behavior probability was proposed.
4. The optimized algorithms based on the Bi module and WO module were verified.
5. The optimal combination of input system and training algorithms was proposed.

# 1 Introduction

## 1.1 Background

The escalating global energy crisis coupled with mounting environmental concerns has thrust the need for sustainable cities and societies into the spotlight. Buildings significantly contribute to this issue, accounting for more than one-third of total global energy consumption [1]. In the United States and the European Union, the percentage of building energy consumption in total energy consumption exceeds 40% [2], and in China, it constitutes 45.5% of the national energy consumption [3]. These figures highlight the pressing need to control building energy consumption and mitigate carbon emissions. Several strategies have been proposed to address this issue including the promotion of distributed energy systems [4], carbon trading mechanisms [5], and smart city construction [6] which needs accurate and online energy consumption predictions. Central to these strategies is the need for accurate real-time energy consumption predictions. Therefore, in recent years, forecasting the electricity consumption prediction of total building, air-conditioning, and plug loads has gained increasing importance. And the plug loads in this study encompass all electronic equipment plugged into wall sockets [8] including electricity consumption from sockets, lighting, and split air conditionings (ACs). In addition to this, the importance of plug-load energy consumption forecasting is twofold.

On the one hand, plug-load electricity consumption constitutes a significant and seemingly increasing percentage of the total energy use. This increment is, in part, due to the advancements in building envelope technologies leading to decreased energy consumption from the HVAC (heating, ventilation, and air conditioning) systems, while consequently increasing the reliance on plug load and lighting [7]. Some recent studies reveal that plug-load electricity consumption accounts for about 32% of total building energy consumption in residential buildings [7], 30% in office buildings [9], 40% in commercial buildings [8], and 80% in hospital laboratories [9]. Moreover, Prashant Anand et al. [10] reported that plug and lighting loads collectively consume 12–50% of building energy, increasing at an average rate of 0.8% per year. These figures underscore the critical importance of plug-load electricity consumption.

On the other hand, plug load can be used for reducing peak electricity consumption and filling low-use periods [15], because of its flexibility and randomness. For example, occupants can reschedule some power-heavy appliances (such as washing machines) to operate during off-peak hours, saving considerable costs on electricity. Especially, this flexibility can also be applied in the 'PEDF' building (structures equipped with four technologies including photovoltaic [13], energy storage [14], direct current [12–13], and flexibility [11]) for improving energy-use flexibility. Similar conclusions have also been drawn in a project from IEA-EBC (Annex 67 [11], theme: Energy Flexible Buildings).

## 1.2 Relevant research concerning building plug loads

In summary, the role of plug-load electricity consumption in total energy consumption is pivotal, and forecasting plug-load electricity consumption can enhance building flexibility online. Referring to recent research, most studies concerning building plug loads concentrate primarily on three areas:

First, some relevant studies have delved into the factors influencing building plug-load electricity consumption and its significance in relation to total building energy consumption. For example, Kim argued that plug loads significantly affect the actual building electricity consumption, possibly because plug load data mirrors the building occupancy and energy use [16]. Additional studies have analyzed the profile characteristics of the building plug-load electricity consumption [17–18].

Second, some relevant studies sought to develop occupant plug-related behavioral models for building performance simulations or other applications, with most research in this area concentrating on occupant behaviors [19]. These primarily involve forecasting or determining the operation schedule and rate of building

plug loads [20–21]. Moreover, a handful of recent studies concerning human dynamics [22–23] have introduced innovative modeling methodologies.

Finally, some relevant studies focused on energy-saving strategies for building plug loads. As summarized by Kamilaris [24], the main categories are 'Software and applications', 'hardware and systems', 'suggestions and advice', and 'affecting the occupants'. Under software measures, they mainly use power management software to adjust and display brightness and standby time, and employ virtual hosting or other strategies to reduce the quantity of office equipment. Hardware measures primarily encompass the use of plugs capable of monitoring and controlling energy consumption, as well as the replacement of some devices with energy-efficient alternatives. Other studies have also explored energy efficiency by manipulating plug-related behaviors [25–26].

Apart from the above-mentioned focus, a limited number of studies have dealt with forecasting building plug-load electricity consumption, particularly via data-driven methods [27–28]. These studies acknowledge the advantages of using time-based neural networks commonly, such as LSTM and its upgraded versions (such as Bi-LSTM). However, there remains potential for further development and optimization of these algorithms. Moreover, the standards for input feature selection are not reasonable and clear. Therefore, the purpose of this study is to further develop the research on building plug load, particularly focusing on the development of improved electricity consumption prediction methods and the discussion on suitable selection criteria for different input features and algorithms.

### 1.3 Relevant research concerning building electricity consumption prediction

This study reviewed various notable research within the energy consumption prediction sphere. Building energy consumption typically manifests through three primary methods.

One method employs physical modeling, which relies on software such as Energyplus. This method models building based on setting building envelope, occupancy schedules, energy-consuming device schedules, and other information in the software for simulation. For example, Giorgio et al. [29] used an energy system model built with Dymola–Modelica and EnergyPlus models to conduct thorough energy modeling and optimization. Veronika et al. [30] used EnergyPlus to investigate the energy baselines of residential buildings. Physical modeling facilitates comprehensive analyses of each energy load, such as lighting, heating, and cooling systems. However, the physical modeling method, despite being widely applied in various applications such as building renovation studies, may not be suitable for the plug load electricity consumption prediction, because it exhibits a specific degree of periodicity [31], while the plug load electricity consumption usually has strong randomness which is strongly influenced by the free and random behavior of occupants [32]. Furthermore, the accuracy of physical modeling methods may be frequently less than ideal [33]. Although optimization methods can improve accuracy (such as using Bayesian estimates for optimization [34]), they often incur higher costs and have extra limitations. Finally, applying physical modeling methods in real-time, online settings may prove challenging, therefore restricting their use in real-time energy consumption predictions during the operational phase of the building.

The other method is the data-driven method, contingent on the selection of appropriate input features and algorithms. The input features of data-driven prediction methods [35] usually incorporate aspects such as building physical performance (for example, thermal characteristics of the building envelope), outdoor meteorological data, indoor environmental data, time, historical energy consumption data, and occupation-related parameters. Besides input features, another crucial aspect of the data-driven method may involve selecting suitable algorithms that can efficiently train the energy consumption prediction model. Previous studies suggested that support vector machines (SVM), artificial neural networks (ANN), decision trees (DT), and other statistical algorithms have extensive applications in data-driven building energy consumption

prediction [36]. Overall, on the one hand, about 47% of studies used ANN, 25% employed SVM, and only 4% used DT to train their models. On the other hand, 24% of the studies employed statistical algorithms such as multiple linear regression (MLR), ordinary least squares regression (OLS), and autoregressive integrated moving average (ARIMA). Compared with the physical modeling method, although most data-driven prediction models operate as black boxes, necessitating additional processes to identify appropriate input features and develop appropriate algorithms, their online application and short-time-scale forecasting capabilities make them a popular choice for energy consumption prediction in the building operation stage.

The final method is the hybrid method. Some studies combine physical modeling methods and data-driven methods [37] to develop a gray-box hybrid model. These models typically perform better than simple white-box and black-box models. However, challenges still exist, such as a lack of clear theoretical hypotheses, standard naming rules, component order determination within the gray-box model, and a unified software solution [37–38]. Moreover, the utilization of software can adversely impact online application performance. Considering the target of this study, only data-driven methods are considered due to their ability for online applications on an hourly scale.

**1.4 Challenges in forecasting plug-load electricity consumption**

Considering the application scenario, this study predominantly employed a data-driven method. Central to data-driven methods is the selection of suitable input features and algorithms. Therefore, the challenges in forecasting plug-load electricity consumption fall into two categories.

First, for input selection, the input features that can be applied in the overall building energy consumption prediction may not be applicable in the plug load electricity consumption prediction.

On the one hand, there are complexities of input selection introduced by the inconsistency in plug-load across different architectural contexts. In other words, the optimal inputs, algorithms, boundary conditions, etc. may not be the same when predicting the electricity consumption of different types of plug loads. The plug loads may have many different categories. For instance, buildings with centralized HVAC systems often isolate pumps and water chilling units in individual rooms, keeping them on a separate electrical branch. On the contrary, buildings without centralized HVAC systems such as some office buildings, generally connect split ACs to the standard wall sockets during the construction process (such as Figure 1). instead of being connected to a separate circuit branch for the HVAC system, which makes the plug load in these buildings include the split air conditioning. As a result, the scope of plug-loads becomes ambiguous which complicates the prediction of plug-load energy consumption. This phenomenon (the item of energy consumption is not clear) has also been found in many studies [39–40]. Therefore, in this study, four categories of plug loads are identified and delineated as shown in Figure 1. The categorization rests on the connection of various electrical equipment to branch circuits. The first category comprises only sockets in the buildings where each type of plug loads including sockets, lights, and all ACs are clearly connected to separate circuit branches. The second and third categories include lights and split ACs respectively, in addition to sockets. The fourth category unifies all elements including sockets, lights, and split ACs simultaneously. These complexities underscore the difficulty of defining the range of plug-load, thereby rendering the selection of an appropriate input feature a significant challenge, which in turn means that the selection of the underlying algorithm, the optimization algorithm, is challenging.

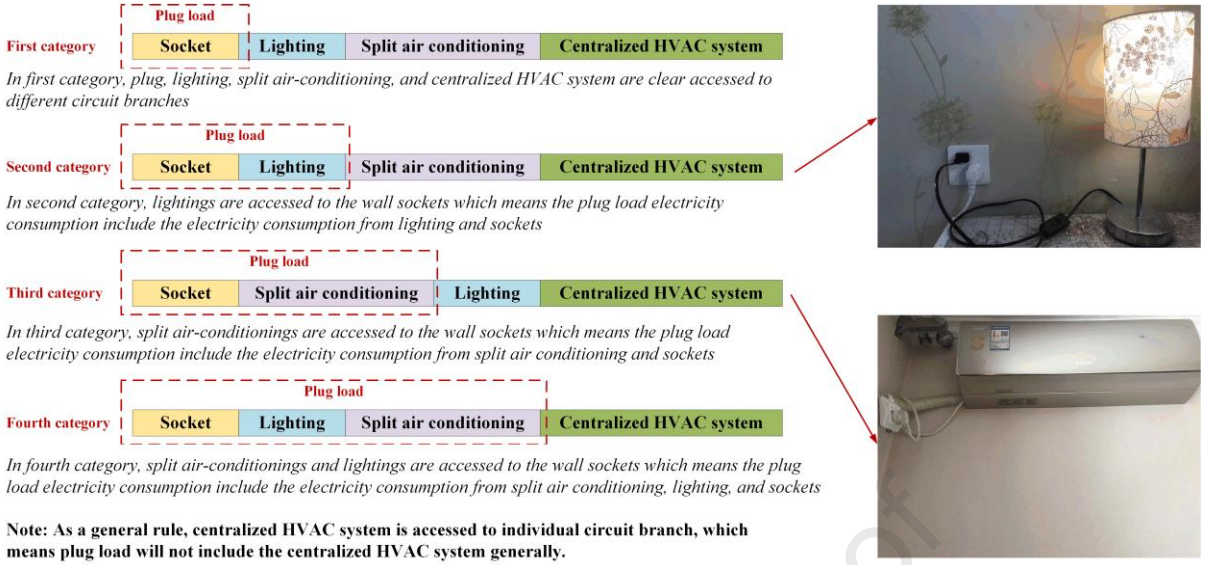


**Figure 1** Four categories of building plug load

On the other hand, another challenge lies in the ambiguity of factors influencing plug-load usage behavior and the consequent electricity consumption. Lighting-related use behavior is strongly dependent on indoor illumination, while AC-related use behavior hinges on indoor temperature. However, plug-related behavior appears random and thus, difficult to predict. Due to the randomness of plug-related behavior, the prediction of this plug-related behavior may be difficult. Activities unrelated to environmental conditions, such as watching television, using computers, and cooking show this randomness. Recent research in human dynamics [22–23] reveals common characteristics in these random behaviors. Most tasks were performed quickly, and a few of them experienced a very long waiting time. That is, these behaviors usually occur repeatedly in the short term and then enter a long-term state of no behavior [22–23]. This suggests that the time interval between subsequent usage of plugs may be a defining factor for the prediction of plug-related behavior and plug-load electricity consumption. However, given the plethora of plugs in a building and the variability in their usage (watching TV, using the washing machine, etc.), recording and incorporating this factor (time interval) into relevant studies might be daunting. To sum up, determining the influencing factors of plug-load electricity consumption remains an unfathomable challenge. The inability to determine the influencing factors means that it is difficult to find the optimal inputs, which in turn means that the selection of the underlying algorithm, the optimization algorithm, is challenging.

Second, for algorithm selection, the algorithms and optimizations need to be further improved. Many kinds of algorithms have been verified for their feasibility [36]. For example, several types of ANN such as Back Propagation Neural Networks (BPNN), Recurrent Neural Networks (RNN), Convolutional Neural Networks (CNN), and their variants including LSTM, Gated Recurrent Unit (GRU) have been explored. Other methodologies such as SVM, Statistical Regression including MLR, ARIMA, DT, and Genetic Algorithm (GA) have also been utilized. Moreover, some recent studies combined many kinds of the above algorithms as a novel algorithm used for forecasting energy consumption. Referring to the related study [36], it appears that ANN has gained preeminence, accounting for approximately 47% of the studies. Notwithstanding, noteworthy challenges still loom, and Figure 2 elucidates this algorithm advancement process including the challenges and solutions. Given the necessity of long-period and short-time-scale prediction outlined in this study, this investigation employs LSTM as the fundamental algorithm. However, some important challenges may still exist. Such challenges include the synchronous consideration of the historical and future state influencing the current state, and the expeditious discovery of the hyperparameters

(weights, thresholds, etc.) optimum solution of neural networks while concurrently enhancing prediction accuracy. To address these issues, this study supplants LSTM with Bi-LSTM for simultaneous consideration of historical and future states. Additionally, a swarm intelligence optimization process is introduced to rapidly pinpoint optimal solutions, circumvent iteration traps in local minima, and enhance prediction accuracy. Figures 2 and 3(b) expound on these details.

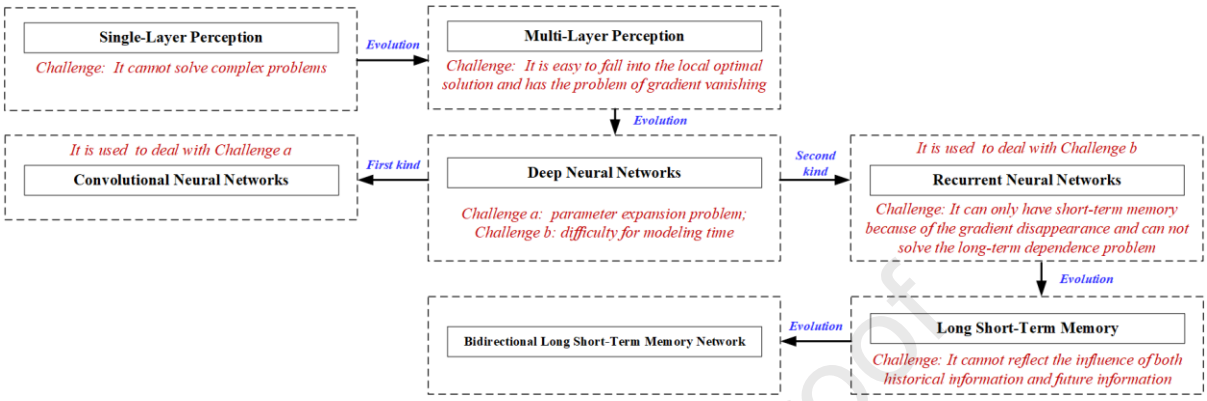


**Figure 2** The upgrading and optimization process of different neural networks

### 1.5 Targets and research framework

In summary, this study introduces a building plug-load electricity consumption prediction system, which employs Bi-LSTM enhanced by swarm intelligent optimization and various input systems for different databases, accuracy requirements, and building types.

First, this study suggests two distinct input systems tailored for varying application scenes. The conventional input system encompasses the determinants of plug-load electricity consumption as prediction input features, whereas the novel inputs system harnesses the probabilities of socket-related behavior and historical electricity consumption as input features, driven by human dynamics theory. The former finds broad application, having been extensively validated, while the latter introduces the probability of occupant behavior to better reflect the real-time human-environment-energy interactions. These two input systems require different data, have different advantages, and can be deployed across diverse energy prediction scenarios.

Second, the forecasting potential of Bi-LSTM and LSTM as the foundational training algorithms is investigated. The advantage of Bi-LSTM over LSTM resides in its broader grasp of time series data context. Specifically, the Bi-LSTM model assimilates both antecedent and subsequent data flows, thus affording a richer sequence analysis potential, instrumental in optimizing prediction performance.

Third, the WO algorithm [41], one of the swarm intelligence optimization algorithms, is introduced as a strategy to improve prediction performance. Further upgradation of WO is achieved by integrating it with circle mapping, one of the chaotic mappings [42–43], thus maintaining population diversity and yielding superior optimization. Moreover, an adaptive weight adjustment process is incorporated into WO.

Finally, this study proposes a selection criterion for the most suited combinations considering building type, data base, and precision requirements, by comparing the applicability and preference of different input features and algorithms.

The detailed main contents of this study are shown in Figure 3(a), and the comparison of the traditional prediction system and upgraded prediction system is presented in Figure 3(b).

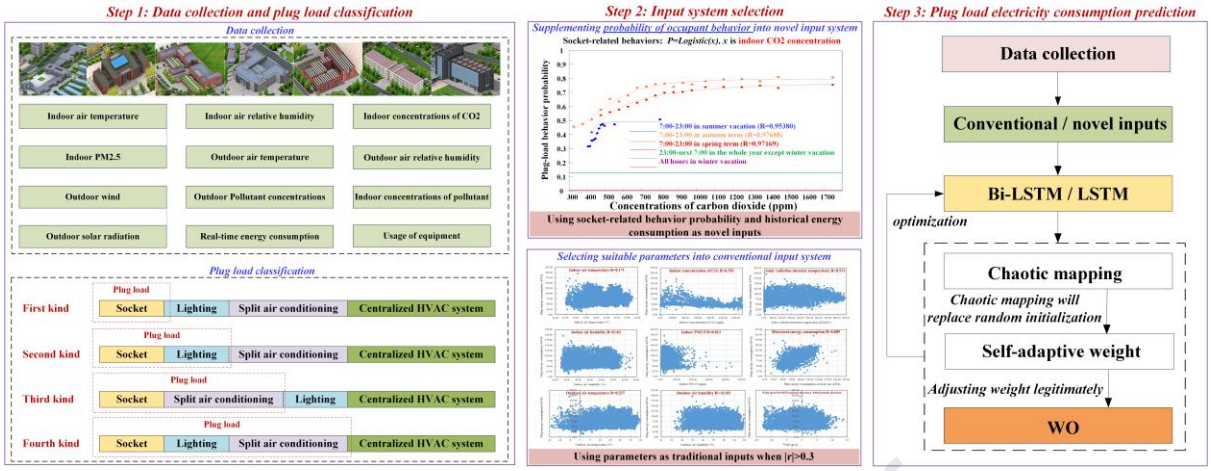


225

226 **Figure 3(a)** The main research contents of this study

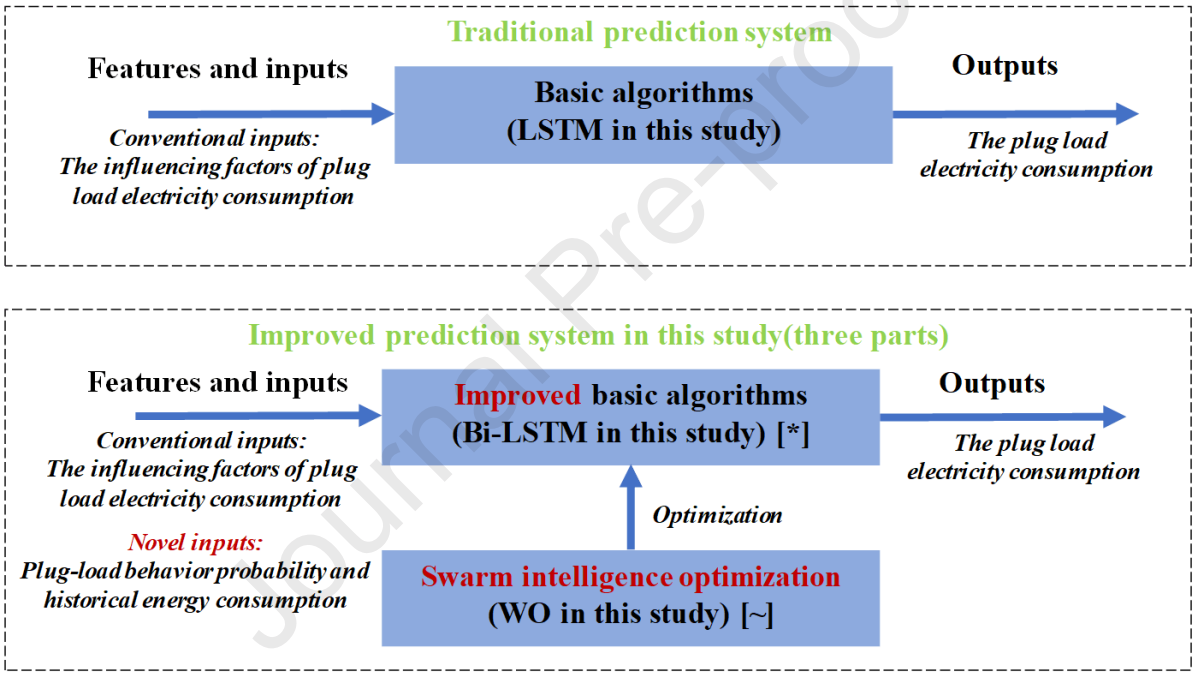


[~] It will find the optimal solution of the neural network more quickly with improving the prediction accuracy simultaneously; In addition, WO prevents iteration from falling into local minima.
[*] It will simultaneously consider the historical and future state which affecting the current state and improve the prediction accuracy

227

228 **Figure 3(b)** The comparison of the traditional prediction system and upgraded prediction system in this study

229 **Figure 3** Targets and works in this study

230 The subsequent sections of this study are as follows. Section 2 introduces sample building, related data
231 collection, plug-related behavior modeling method, and the process involving the Pearson correlation
232 coefficient method, Bi-LSTM, LSTM, and improved WO. Section 3 shows the results derived from different
233 input systems and algorithms. In Section 4, the comparisons of prediction results from different input features
234 and algorithms, including an exploration of the suitability and preference of different combinations, are
235 discussed. Section 5 encapsulates the conclusions.

236 **2 Methodology**

237 **2.1 Sample buildings**

The focal point of this study incorporates seven buildings with diverse functionalities and plug loads to explore the determinant factors of plug- load electricity consumption. Another facet of scrutiny is enhancing prediction performance utilizing LSTM or Bi-LSTM in tandem with improved whale optimization algorithms. A compendium of these buildings' specifics can be found in Table 1 with corresponding façades exhibited in Figure 4.

**Table 1** Specifications of seven typical buildings

| No. | Types | Energy system | Plug-load categorization | BEUI (kWh/a·m$^2$) | Opened time in a day | Opened day in a year |
|---|---|---|---|---|---|---|
| A | Office | Sockets, lighting, centralized variable refrigerant flow ACs | Second | 44.89 | Opened: All 24 hours | Opened: All 365 days |
| B | Laboratory | Sockets, lighting, split ACs | Fourth | 75.76 | Opened: All 24 hours | Opened: All 365 days |
| C | Library | Sockets, lighting, centralized ACs | Second | 30.54 | Opened: 7:00–23:00<br>Closed: 23:00–next 7:00 | Opened: other days<br>Closed: winter vacation |
| D | Library | Sockets, lighting, centralized ACs with water chiller in most areas, and split ACs in some other rooms | Fourth | 60.09 | Opened: 7:00–23:00<br>Closed: 23:00–next 7:00 | Opened: other days<br>Closed: winter vacation |
| E | Education building | Sockets, lighting, variable refrigerant flow ACs | Third | 62.74 | Opened: 7:00–23:00<br>Closed: 23:00–next 7:00 | Opened: other days (summer, spring, and autumn term)<br>Closed: winter vacation |
| F | Education building | Sockets, lighting | Second | 37.76 | Opened: 7:00–23:00<br>Closed: 23:00–next 7:00 | Opened: other days (summer, spring, and autumn term)<br>Closed: winter vacation |
| G | Office | Sockets, lighting, centralized ACs | Second | 41.55 | Opened: All 24 hours | Opened: All 365 days |

Note: The Building Energy Use Intensity (BEUI) refers to the annual energy consumption per unit of building area in a building, providing an assessment of the overall energy consumption level of the building.

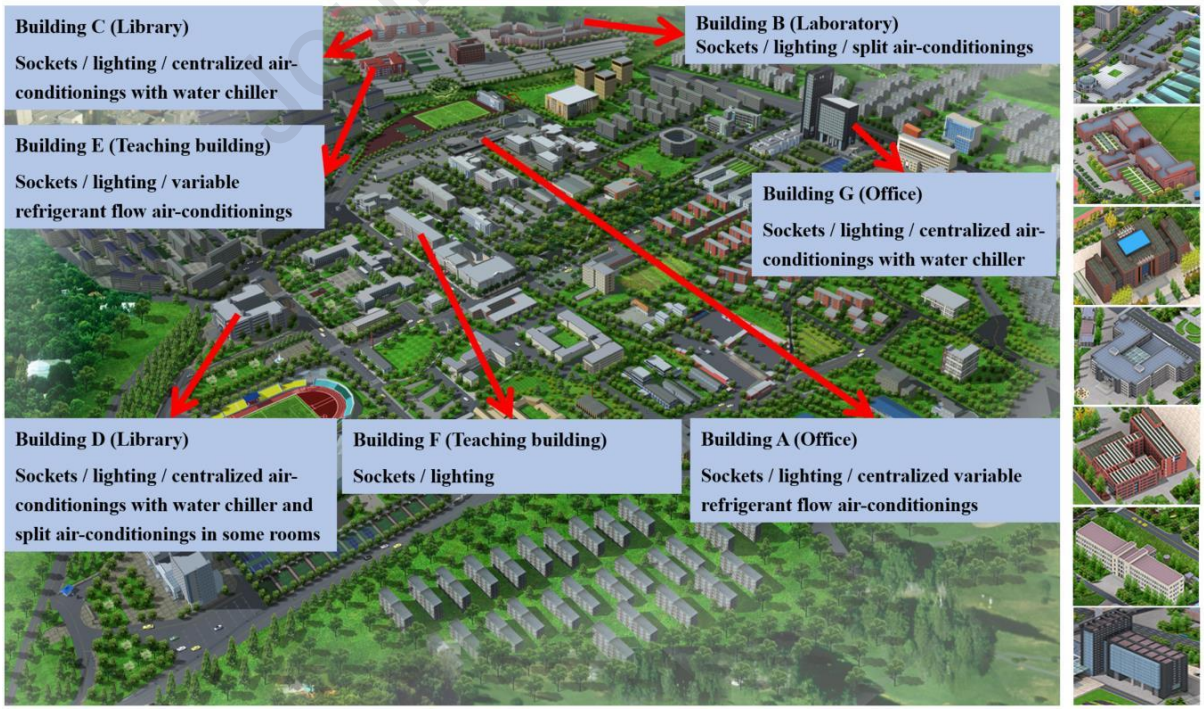


**Figure 4** Sample buildings in this study

## 2.2 Data acquisition

Recent studies [35, 44] suggest the incorporation of varied data types, encompassing outdoor meteorological factors, indoor environmental parameters, time, historical energy consumption, and occupant-related parameters. The occupant-related data generally comprise occupancy and the number of occupants [27, 44]. However, monitoring occupants poses significant challenges. It may infringe privacy violations if intrusive, or necessitate an extensive sensor network which needs additional costs such as PIR (Passive Infra-Red) sensors [45], if non-intrusive. Moreover, achieving comprehensive coverage of the sample buildings for an 8760-hour period enhances the complexity of occupant monitoring. Therefore, in this study, $CO_2$ concentration data will serve as an approach to illustrate the number of occupants, superseding direct occupancy tracking. Similar strategies have been utilized in some other studies, translating $CO_2$ concentration data into occupant-related data using methods including decision tree [47], logical inference [47], random forest [46], support vector machine [46], change point analysis [48], etc. Therefore, this study requires electricity consumption data (comprising historical electricity consumption and usage for the previous hour, and the duration of the plug usage including the commencement and cessation times), indoor environmental data (comprising indoor air temperature, $CO_2$ concentration, air humidity, and PM2.5 concentration), and outdoor meteorological data (comprising solar radiation intensity, outdoor air temperature, air humidity, and wind speed).

Concerning data acquisition, first, for electricity-related data, an energy-consumption monitoring system was installed in the sample buildings and has operated successfully for several years, establishing a cloud platform for recording, as shown in Figure 5(a). This system can accurately record the real-time expression values of all electrical branches in every room. Second, indoor environmental data were collected through ceiling-mounted sensors positioned within the buildings (excluding stairwells) as shown in Figure 5(b), with at least one sensor per room. Finally, outdoor meteorological data were extracted from the public dataset maintained by the China Meteorological Science Data Center (http://data.cma.cn) [49]. All compiled datasets collected data at hourly intervals throughout the year 2021.

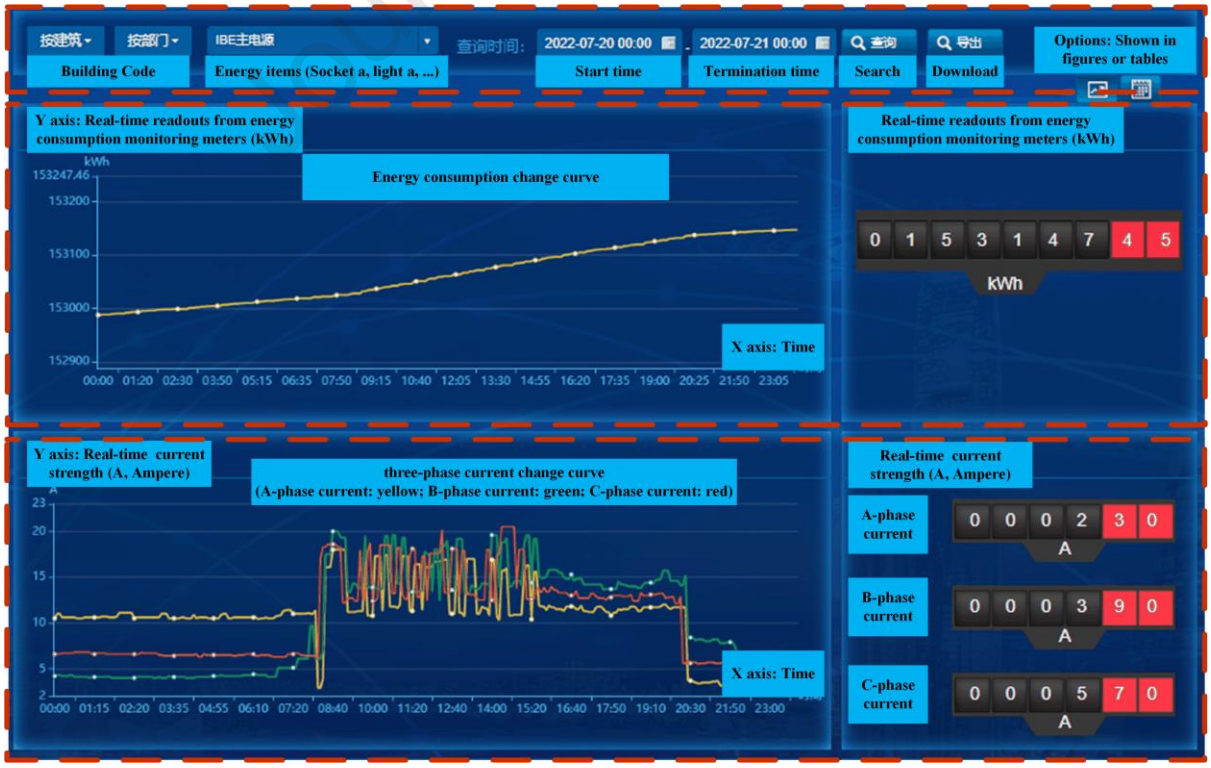

**Figure 5(a)** Energy-consumption monitoring platform (original figure and translation)

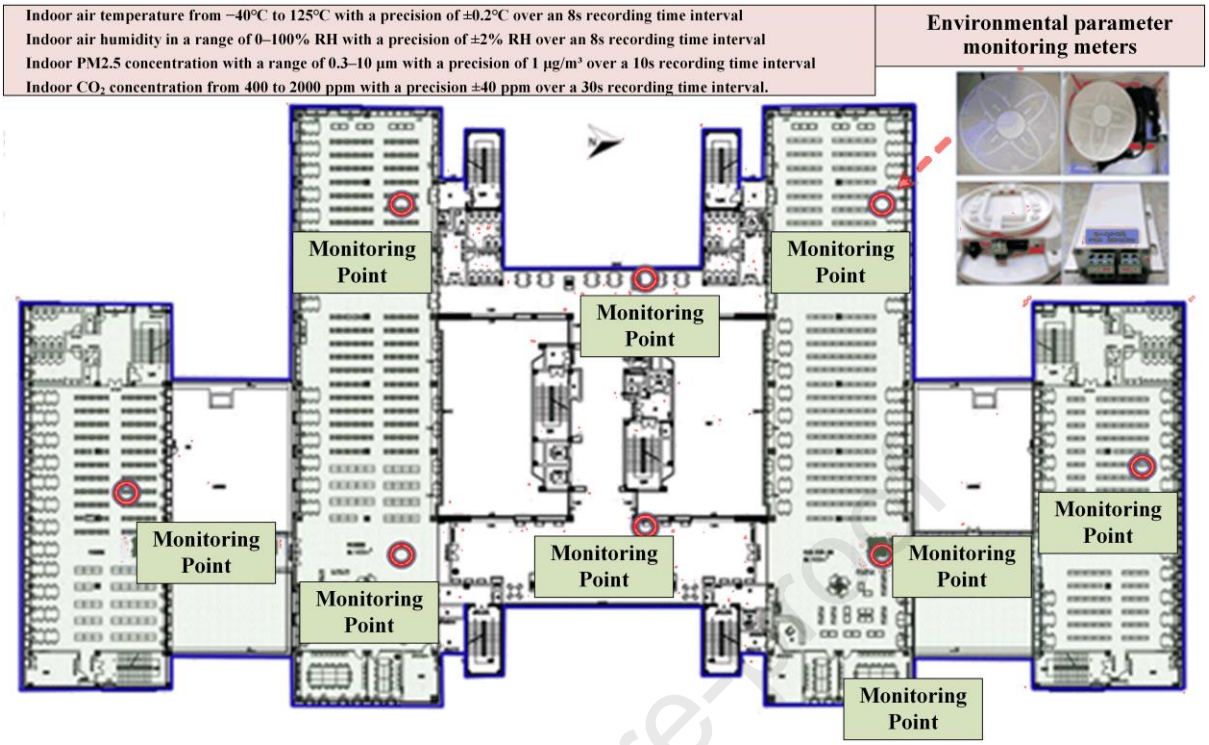


**Figure 5(b)** Indoor environment sensor measuring points

**Figure 5** Related data acquisition by different sensors or platforms

### 2.3 Input system modeling and selection

Figure 3 and the Introduction allude to the formulation of two distinct input systems catering to different application scenarios as a point of focus for this study.

The conventional input system will be leveraged. This system operates based on the identification of varying parameters that influence plug load electricity consumption, which subsequently functions as input features. The unclear categorization and ambiguous determinants of plug loads necessitate the analyses of an assortment of parameters via the Pearson correlation coefficient method elucidated in Section 2.3.1.

Contrary to the conventional system, the novel input system builds upon some recent studies [22–23] into human dynamics within buildings. Eschewing the broad spectrum of plug loads and forsaking the use of pertinent factors, this system utilized historical plug-load electricity consumption, combined with the probabilities of plug-load behaviors to create a unique input system. A comprehensive description of methodologies employed to model plug-related behaviors will be presented in Section 2.3.2.

#### 2.3.1 Pearson correlation coefficient method

In the quest for rational input features, the core factors influencing energy consumption and utilization are typically assimilated as input parameters. The correlation coefficient '*r*' is a prevalent metric for ascertaining these influences. That is, the stronger the correlation ('*r*' is larger) indicates that the parameter is more strongly correlated with energy consumption and is more suitable as an input for energy consumption prediction. Referring to recent studies and analyses in this study, parameters to be considered encompass electricity-related data (historical electricity consumption an hour ago), indoor environmental data (indoor air temperature, $CO_2$ concentration, air humidity, PM2.5 concentration), outdoor meteorological data (solar radiation intensity, outdoor air temperature, air humidity, wind speed), and occupant-related data (using $CO_2$ concentration replacing the number of occupants). Equation (1) delineates the Pearson correlation coefficient method where the correlation coefficient '*r*' arbitrates the degree of linear correlation between variables.

$$r = \frac{\sum_{i=1}^{n}(x_i-\bar{x})\times(y_i-\bar{y})}{\sqrt{\sum_{i=1}^{n}(x_i-\bar{x})^2\times(y_i-\bar{y})^2}} \quad (1)$$

Where, $r$ is the correlation coefficient of variables $x$ and $y$, with its values oscillating between -1 and 1 inclusively. This study assigns $y$ as the plug-load electricity consumption, and $x$ echoes the parameter outlined previously. Conventionally, correlation potency is designated as follows, 'r=0' signifies no correlation, '0 <|r|≤0.3' indicates a weak correlation, '0.3 <|r|≤0.5' indicates a low correlation, '0.5 <|r|≤ 0.8' indicates a significant correlation, '0.8 <|r| < 1' indicates a high correlation, and 'r=1' indicates a perfect linear correlation, as cited by references [50–51]. However, these thresholds remain arbitrary, and situational adjustments may apply. In the realm of building energy research, many studies have scrutinized how environmental parameters and temporal characteristics influence building energy consumption and usage, encompassing indoor and outdoor air temperature, humidity, sunshine duration, and ventilation rate [50–51]. Based on the above research, valid correlations (that is, the parameter can be used for energy consumption prediction input features) are usually expressed as the correlation coefficient typically ranges from 0.3 to 0.5. Therefore, if the correlation coefficient exceeds 0.3, the corresponding parameters will be deemed as potential input features in this study.

### 2.3.2 Defining and modeling plug-related behavior probability

Building energy consumption is significantly influenced by occupant behavior, as corroborated by numerous pertinent studies. Generally, mathematical modeling of occupant behavior aims to probability of action using a specific model, represented by equation (2). However, this study innovatively supplements this approach, selecting equation (3) as the calculation model.

$$P_{(T_i-T_{i+1})} = \frac{\sum_{j=1}^{n} M_j}{n\times M_0} \quad (2)$$

$$P_{(T_i-T_{i+1})} = \frac{\sum_{j=1}^{n} \Delta T_j}{n\times \Delta T_0} \quad (3)$$

Where, $i$ is a time index (e.g., if $i$ is 8, then $T_{i-1}, T_i,$ and $T_{i+1}$ correspond to $T_{7:00}, T_{8:00},$ and $T_{9:00}$, respectively); $j$ represents each socket and $n$ is the total number of sockets (e.g. if a building has 100 sockets, then $n$ = 100, with $j$ numbered from 1 to 100); $M_0$ and $M_j$ represent the times of the plug-related actions and total actions respectively. $\Delta T_0$ represents the time difference between $t_n$ and $t_{n+1}$ (where, in this study, $\Delta T_0$ is 1 hour); while $\Delta T_j$ represents the usage time of the $j$th socket during the period from $t_n$ to $t_{n+1}$. Moreover, $t_n$ and $t_{n+1}$ represent the start and end times respectively (in this study, the starting and ending moments are all integral hour points, such as 0:00, 1:00, etc.).

Historically, the traditional occupant behavior probabilities were calculated by employing the ratio of the total number of a specific action to the total number of all actions. Improving this conventional method, the proposed probabilistic model determines probability based on the duration ratio of certain actions to the total duration. Building upon foundational literature pertaining to occupant behavior modeling (refer to Equation 3), this innovative concept is introduced (refer to Equation 2). To elucidate the differences between Equations (2) and (3), considering the following example when it needs to predict plug-load energy consumption from 13:00 to 14:00, Scenario A envisions occupants sparking plug-load use at 13:01 persisting until 14:00, while Scenario B envisions it commencing at 13:59 and enduring until 14:00. Specifying the 13:00 to 14:00 time frame, traditional method (equation 2) would imply a constant occupant behavior probability of 1 (1/1) that fails to discern between Scenarios A and B. Conversely, the proposed equation (equation 1) implies disparate occupant behavior probabilities of 1/60 and 59/60 for Scenario A and B, respectively that is successful to discern between Scenarios A and B.

With its unique advantages, this change contributes to a richer understanding of energy-consuming

equipment use. First, it better accentuates the intensity of energy use. Secondly, it provides flexibly in modeling probabilities at different time-scale levels, such as hourly, daily, or monthly behavior probabilities. The traditional method tends to fail when modeling probabilities at an hourly time-scale or below, as the low likelihood of repeated identical energy-use behaviors within a single hour (e.g., turning on a light 5 times and then turning it off 4 times within an hour would constitute a low probability event). Therefore, the proposed method (equation 3) resonates with energy consumption studies more by emphasizing the intensity and duration of energy-consuming equipment usage duration and magnitude rather than the identity of the operators (e.g., using equipment during 13:00-13:30 by occupant A, and using it during 13:30-14:00 by occupant B would yield similar energy consumption during 13:00-14:00). However, it is crucial to mention that the proposed model (equation 3) may be less suitable for applications such as thermal comfort modeling, precise behavior modeling, etc., where cases needs the distinctions of occupants, time, and additional variables.

To calculate equation (3), there are primarily two methods. The first employs random models to encapsulate the diversity evident in space, time, and occupant behaviors, while the second utilizes statistical models. The Markov model and its variants may be the most popular among random models. Despite their prevalence, the complexity of their solving and modeling tools translates into weak online application capabilities. Furthermore, as indicated in IEA EBC-Annex 66 (Definition and Simulation of Occupant Behavior in Buildings [60]), studies suggest that stochastic models to capture spatial, temporal, and individual diversity do not necessarily perform better than simplified deterministic models. Therefore, the focus of this study is the application of statistical models for deciphering equation (3). Reviews of recent studies reveal a challenge in identifying suitable physical parameters for use as independent variables in plug-load-related behavior probability, different from indoor air temperature to AC-related behavior and indoor illuminance to lighting-related behavior. Nevertheless, with advances in human dynamics theory [22–23], it has been illustrated that most random tasks are performed quickly, and a few of them have experienced very long waiting time. That is, random behaviors usually occur repeatedly in the short term and then enter a long-term state of no behavior. Thus, it can be inferred that the historical energy-use behavior situations can serve as a predicting or exerting influencing factor on the real-time random behavior within a few proximate hours. As a result, the probability of plug-load behaviors can be expressed as in equation (4).

$$P_{(T_i\text{-}T_{i+1})} = f(some\ uncertain\ factors) = f(u_{i-1}) \quad (4)$$

Where, $u$ is the influencing factor, and $i$ is a time index similar to Equations (2–3). Although there lacks consensus regarding the exact influencing factors, some researches proposed some parameters such as the waiting time from the last action to the current action referring to human dynamics theory [22–23], indoor $CO_2$ concentration [44], and psychosocial elements such as attitudes and personal norms [52]. Moreover, the mapping function ($f$) akin to equation (6), commonly incorporates statistical models [22, 54–55] (such as logistics, quadratic, sigmoid, and probity functions), fuzzy functions [52], and even some machine learning algorithms [53]. In this paper, the influencing factor ($u$) selected is the indoor $CO_2$ concentration, and the mapping function will be fitted to actual measuring data.

### 2.4 Process and principles of algorithms

#### 2.4.1 LSTM and Bi-LSTM

The Introduction phase refers to multiple algorithms utilized for neural networks such as Back-propagation neural networks. However, the particular necessities encompassing long period and short time-scale prediction proposed in this study, necessitate the deployment of a time sequence neural network. Therefore, in this study, LSTM and Bi-LSTM, two extensively employed time sequence neural networks,

will be selected to function as the principal algorithms. The commonly-used time sequence model structures include the Prophet, ARIMA, LSTM, Transformer, and Informer. However, the Prophet toolkit is suitable for predicting trends whereas it is unsuitable for predicting values, especially when facing long sequence problems. ARIMA even battles with inaccuracy in trend prediction. Moreover, Transformer and Informer are very recently proposed and are yet to be completely evaluated. Therefore, in this study, the LSTM and its variant Bi-LSTM, the most classical time sequence neural network, will be selected. The construction of LSTM and Bi-LSTM is shown in Figure 6.

In this study, the distribution of training to test sets assumes a ratio of 7:3. Presented inputs and outputs undergo a normalization process. When the number of inputs is assigned the variable $m$, the number of hidden layers will be calculated as ($2m$+1). Moreover, both Bi-LSTM and LSTM are designed with a maximum number of iterations (MaxEpochs) of 1000, and an initial learning rate (InitialLearnRate) of 0.01. The LearnRateDropPeriod is 800, and the LearnRateDropFactor is 0.8 implying that the learning rate is multiplied by this factor every 800 periods. To counteract potential overfitting in Bi-LSTM and LSTM, L2 Regularization is implemented [56]. Moreover, traditional batch gradient descent can be computationally intensive, while stochastic gradient descent may not converge easily. Thus, this study also resorts to Mini-batch gradient descent. For LSTM, the MiniBatchSize is set to 240 for LSTM (that is the size of the mini-batch, and the MiniBatchSize typically represents a multiple of 2 between 0 and the maximum number of iterations).

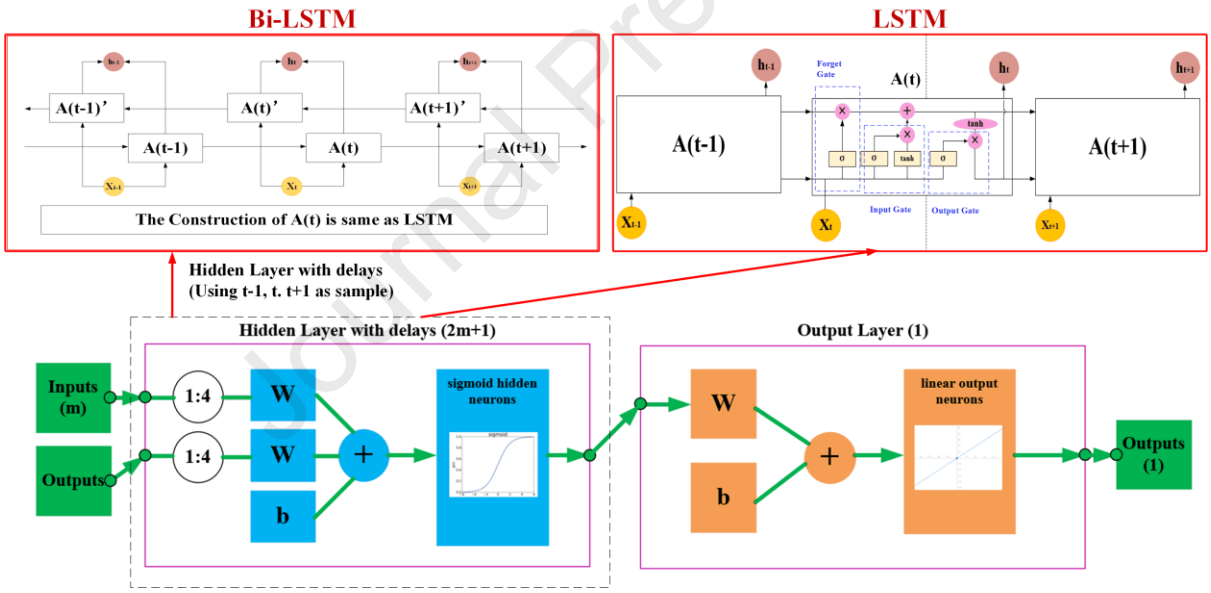


**Figure 6** The construction of LSTM and Bi-LSTM

### 2.4.2 WO algorithm with circle mapping and self-adaptive weight adjustment

According to Section 1 (Introduction), to improve the prediction performance, including finding the optimal solution identification for hyperparameters of neural networks such as weights and thresholds, prevention of convergence into local minima, and boosting prediction precision. Some recent studies have attempted to use swarm intelligent algorithms for optimization [57–58], such as Grey Wolf Optimization (GWO), Harris-Hawks Optimization (HHO), WO, Bald Eagle Search (BES), Manta Ray Foraging Optimization (MRFO), Sparrow Search Algorithm (SSA), Grasshopper Optimization Algorithm (GOA), and Bat Algorithm (BA). However, the unique characteristics of each algorithm lead to variable results. For instance, Li et al. [57] used 22 standard test functions to compare various swarm intelligent algorithms and revealed differing outcomes in terms of convergence speed, accuracy, and stability. SSA (proposed in 2020)

emerged as the overall superior performer, followed by WO (proposed in 2016) and GWO (proposed in 2014), while BA (proposed in 2010) and GOA (proposed in 2017) manifested relatively weaker performance. Similarly, in a comprehensive comparison of 43 population intelligence algorithms, Zhang et al. [58] reported that BES (proposed in 2020) showcased stellar performance, while WO, HHO (proposed in 2019), MRFO (proposed in 2019), and other algorithms and their quadratic optimization also have good performance. However, these results are highly context-dependent, and swarm intelligence algorithms can also be further optimized. Therefore, it seems a significant challenge to directly determine the superiority of one swarm intelligent algorithm across energy consumption prediction scenarios. Given these constraints, the algorithm selection for this study accounted for optimization performance (refer to the research of Li, and Zhang), age of invention (older designs might show reduced performance while recent designs may not yet have extensive research support), and the complexity of the algorithm. Consequently, WO was selected as the optimization algorithm for its advantageous balance of these factors. However, it is worth noting that WO is not without limitations. Therefore, to augment WO optimization capabilities, it is proposed that WO incorporates adaptive weight adjustment and population initialization modules. These advancements can accelerate convergence speed, diversity population, calculate suitable weights, and ultimately enhance prediction accuracy.

Introduced by Mirjalili et al. [59], WO derives inspiration from the social hierarchy and hunting behavior of the whales. The whales swarm around their prey, exuding bubbles as they spiral, creating a spiral "bubble web" that pushes the prey closer together. This process can be divided into three parts [59], as visually depicted in Figure 7.

(1) Encircling the prey: Assuming that *N* whales scouring a d-dimension search area, the position of the *i*th whale can be expressed as $X_i = (X_{i1}, X_{i2}, X_{i3}, \ldots, X_{id})$. In the process of searching for prey, the models of approaching and outflanking prey are shown by equations (5–8).

$$(1)\ D = \left|C \times X_p(\mathrm{t}) - X(t)\right| \tag{5}$$

$$(2)\ X(t+1) = X_p(\mathrm{t}) - A \times D \tag{6}$$

$$(3)\ C = 2R_1 \tag{7}$$

$$(4)\ A = 2aR_2 - a, a = 2 \times \left(1 - \frac{t}{T_{max}}\right) \tag{8}$$

Where, *t* indicates the current iteration, while *C* and *A* are coefficient vectors. $X(t)$ and $X_p(t)$ refer to the position vector of a whale and the prey, respectively. $T_{max}$ is the maximum number of iterations, $a$ is a control parameter (whose value, ranging from 0 to 2, decreases linearly with an increase in the number of iterations), and $R_1$ and $R_2$ are random numbers ranging from 0 to 1.

(2) Bubble net attack (exploitation phase): In this part, the predatory strategy bifurcates into two forms.

(2-1) Shrinking encircling mechanism: This process involves a straight-line swim without bubbling.

(2-2) Spiral updating of position: This implies spiraling and bubbling. Assume that there is a 50% probability of choosing between either the shrinking encircling mechanism or the updating of the position of whales during optimization, shown in equations (9–11).

$$X(t+1) = D^* \times e^{bl} \times \cos(2\pi l) + X^*(t) \tag{9}$$

$$D^* = |X^*(t) - X(t)| \tag{10}$$

$$X(t+1) = \begin{cases} X^*(t) - A \times D, & \text{if } p < 0.5, \\ D^* \times e^{bl} \times \cos(2\pi l) + X^*(t), & \text{if } p \geq 0.5. \end{cases} \tag{11}$$

(3) Search for prey (exploration phase): In addition to group hunting, humpback whales also resort to random foraging based on their individual positions. This behavior further deters the algorithm from succumbing to local optimal values. The mathematical model for this behavior mimics that of direct

swimming, articulated through equations (12–13).

$$D^* = |C \times X_{rand} - X| \tag{12}$$

$$X(t+1) = X_{rand} - A \times D \tag{13}$$

Where $D^*$ indicates the distance between the *i*th whale and the prey (the best solution ascertained till that moment). $p$ is a random number in [0,1], $l$ is a random number in [−1,1], and $b$ is a constant for defining the shape of the logarithmic spiral. $X_{rand}$ is a randomly selected position vector (a random whale) from the current population. In this paper, the population quantity is 5 and the maximum number of iterations is 30.

However, for the confines of the initial WO, it utilizes randomly generated data as the foundation of its population information. This method presents challenges in preserving population diversity, subsequently leading to suboptimal optimization results. Therefore, this study seeks to address this issue by introducing chaotic mapping for allowing WO to circumvent local optimal solutions with relative ease, enhancing population diversity, and improving global search capabilities. Moreover, optimization of the neural network weight was accomplished through a self-adaptive weight process specifically tailored for WO, represented in equation (14).

$$w = w_{min} + (w_{max} - w_{min}) \times mm \times \exp\left(\frac{-t}{G_{max}}\right) \tag{14}$$

Where $w$ is the weight with $w_{max}$ being 1 and $w_{min}$ being 0 respectively. $mm$ is the adjustment coefficient and is set to 1 in this study. $t$ is the number of iterations and $G_{max}$ is the population maximum evolutionary algebra.

In summary, the process (main steps) for optimizing Bi-LSTM with WO is shown in Figure 7. The figure presents a flowchart of the process. The input features, outputs, and incorporated improved algorithms are further specified as follows. The output is the energy consumption of plug loads in buildings. For the input system, the data will be used as hourly-time-scale for a whole year. Conventional inputs encompass parameters that possess a correlation coefficient greater than 0.3 with energy consumption. These parameters may include historical energy consumption (the past hour), time, indoor environmental parameters, outdoor meteorological parameters, and the number of occupants depicted by indoor $CO_2$ concentration. Novel inputs proposed comprise data related to occupant behavior probability and historical energy consumption (the past hour). Algorithms include LSTM, Bi-LSTM, LSTM-WO, and Bi-LSTM-WO.

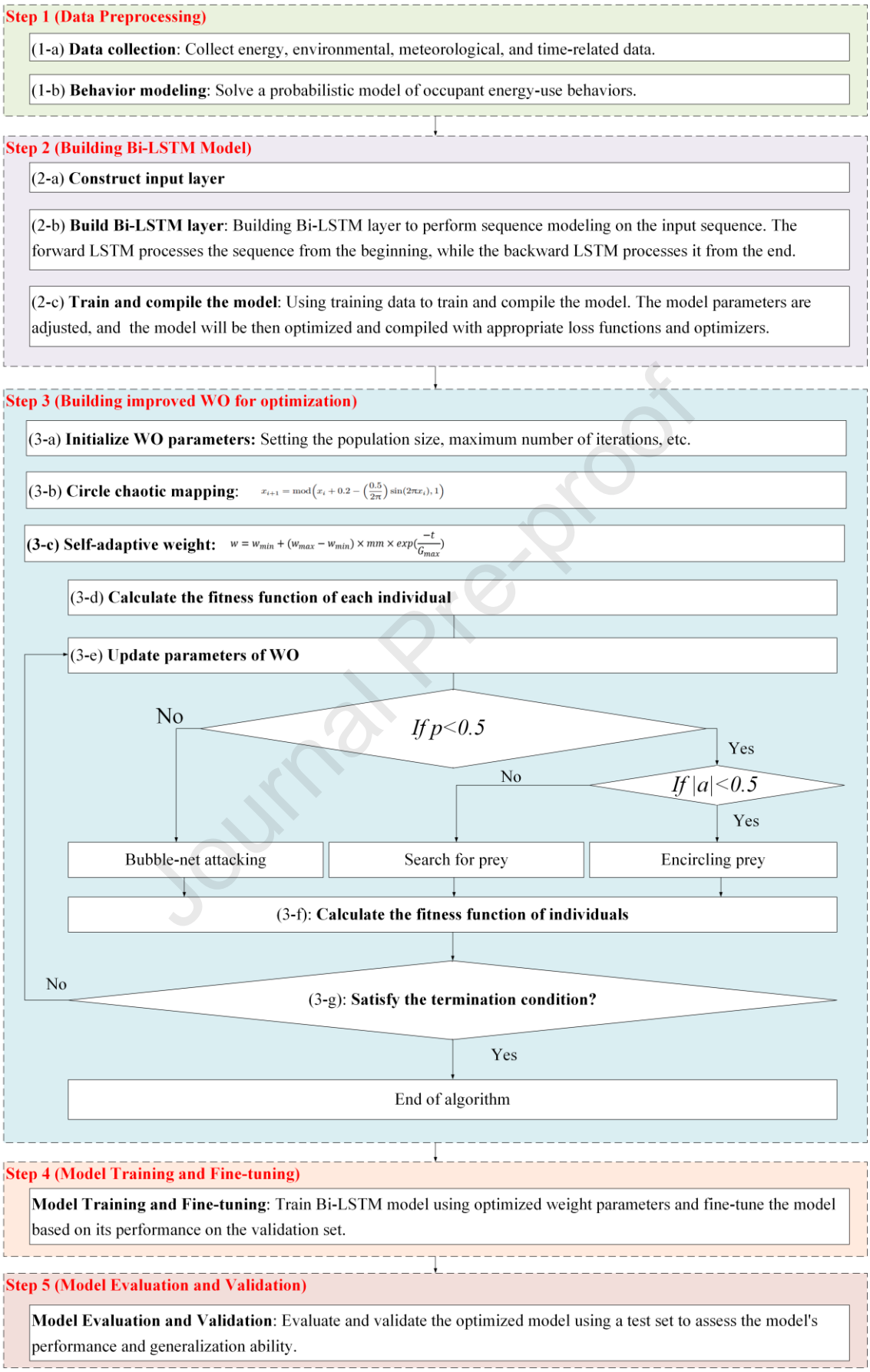


**Figure 7** The flowchart (main steps) for optimizing Bi-LSTM with WO

### 2.5 Evaluation of prediction models

This study employed five evaluation indices for evaluation: the coefficient of determination (R), the mean absolute error (MAE), the mean absolute percentage error (MAPE), the root mean square error (RMSE), and the coefficient-of-variation of root mean square error (CV-RMSE). These indices are formulated as equations (15–19). Each of these evaluation indices offers a distinct perspective on the effectiveness of prediction models. R exemplifies the fitting performance, and MAPE (MAE) outlines the average precision performance. CV-RMSE (RMSE) proves highly responsive to significant deviations in the prediction dataset, effectively capturing dispersion, which will be called the dispersion performance in this study. The better performance includes enhanced accuracy (including better fitting, average precision, and dispersion performance) with less reduced operation time consumption.

$$R\ (E_a, E_b) = 1 - \frac{\sum_{c=1}^{c=n}(E_{a,c}-E_{b,c})^2}{\sum_{c=1}^{c=n}(\bar{E}-E_{a,c})^2} \tag{15}$$

$$MAE\ (E_a, E_b) = \frac{\sum_{c=1}^{c=n}|E_{a,c}-E_{b,c}|}{n} \tag{16}$$

$$RMSE\ (E_a, E_b) = \sqrt{\frac{\sum_{c=1}^{c=n}(E_{a,c}-E_{b,c})^2}{n}} \tag{17}$$

$$MAPE\ (E_a, E_b) = \frac{\sum_{c=1}^{c=n}|\frac{E_{a,c}-E_{b,c}}{E_{b,c}}\times 100\%|}{n} \tag{18}$$

$$CV-RMSE\ (E_a, E_b) = \frac{\sqrt{\frac{\sum_{c=1}^{c=n}(E_{a,c}-E_{b,c})^2}{n}}}{\overline{E_b}} \tag{19}$$

Where, $E_a, and\ E_b$ represent the prediction and actual energy consumption respectively, kWh. In addition, this study introduces a new parameter *PI* (performance improvement) to measure the improvement resulting from enhancing algorithms or using different input features. Expressions for $PI_{RMSE}$, $PI_{MAE}$, $PI_{CV-RMSE}$, and $PI_{MAPE}$ are shown in equation (20), with the equation for $PI_R$ shown in equation (21). According to these two equations, positive and negative values correspondingly indicate performance improvement or degradation.

$$PI_{RMSE,\ or\ MAPE,\ or\ MAE,\ or\ CV-RMSE} = \frac{M_0-M_1}{M_0}\times 100\% \tag{20}$$

$$PI_R = \frac{M_1-M_0}{M_0}\times 100\% \tag{21}$$

Where, $M_0$ and $M_1$ denote the values of the evaluation indices before and after development. For example, if comparing LSTM and Bi-LSTM, the $M_0$ is the performance of LSTM while the $M_1$ is the performance of Bi-LSTM. Similarly, if comparing LSTM and LSTM-WO, the $M_0$ is the performance of LSTM while the $M_1$ is the performance of LSTM-WO.

## 3 Results

Derived from the methodology outlined in Section 2.3, the section presents the energy consumption prediction results using different input features and algorithms.

### 3.1 Results on using the conventional input system

#### 3.1.1 Results on influencing factors of plug-load energy consumption and usage

The preliminary step in utilizing the conventional input system is identifying the influencing factors that contribute to different electricity consumption across different plug loads. Detailed results are shown in Table 2 and Figure 8. In Figure 8, '$|r|$=0.3' is denoted by the blue line, and the parameters surpassing this line are taken into account as significant influencing factors. The conclusions are shown as follows.

**Table 2** Correlation coefficient (*r*) results between plug load electricity consumption and parameters

| Potential input features | Building A | Building B | Building C | Building D | Building E | Building F | Building G |
|---|---|---|---|---|---|---|---|
| Indoor air temperature | 0.171 | 0.462 | 0.092 | 0.698 | 0.351 | -0.006 | -0.189 |
| Indoor $CO_2$ concentration | 0.383 | 0.310 | 0.535 | 0.688 | 0.508 | 0.441 | 0.311 |
| Indoor air relative humidity | 0.162 | 0.489 | -0.119 | -0.580 | 0.416 | 0.043 | 0.052 |
| Indoor PM2.5 concentration | 0.013 | 0.088 | -0.011 | -0.234 | -0.161 | -0.010 | -0.144 |
| Solar radiation intensity | 0.513 | 0.551 | 0.380 | 0.170 | 0.178 | 0.401 | 0.455 |
| Outdoor air temperature | 0.237 | 0.523 | -0.080 | -0.421 | 0.448 | 0.109 | 0.064 |
| Outdoor air humidity | -0.103 | 0.161 | -0.228 | -0.199 | 0.241 | -0.143 | -0.117 |
| Wind speed (Longitude) | 0.007 | 0.220 | -0.059 | -0.202 | 0.161 | -0.010 | 0.041 |
| Wind speed (Latitude) | -0.061 | -0.208 | -0.024 | 0.152 | -0.228 | 0.000 | -0.048 |
| Historical electricity consumption | 0.809 | 0.931 | 0.913 | 0.929 | 0.973 | 0.921 | 0.905 |

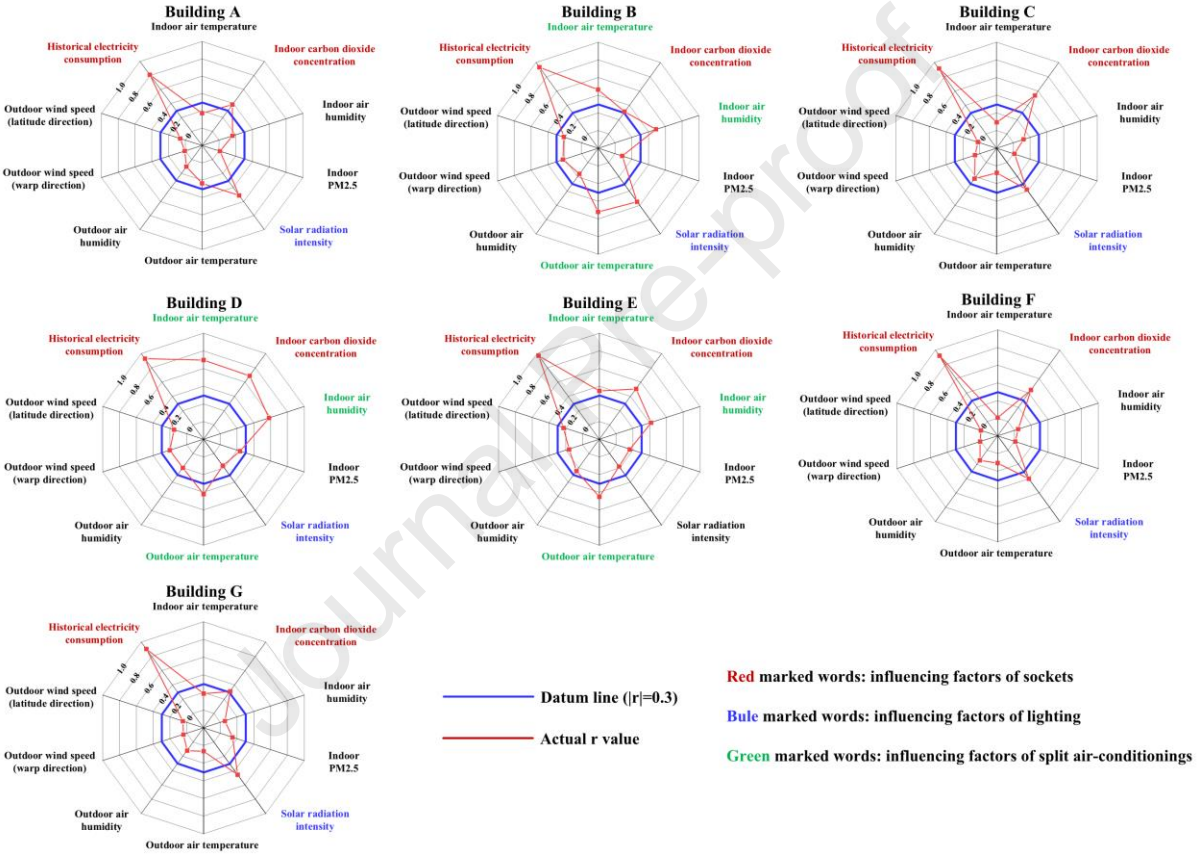


**Figure 8** Correlation coefficient ($r$) results between plug load electricity consumption and parameters

For the second category, comprising Buildings A, C, F, and G, the plug loads encompass the sockets and lighting. It is inferred that the influencing factors include historical electricity consumption, indoor $CO_2$ concentration, and solar radiation intensity.

For the third category, comprising Building E, the plug loads encompass the sockets and split ACs. The influencing factors include historical electricity consumption, indoor $CO_2$ concentration, indoor air temperature, indoor air humidity, and outdoor air temperature.

For the fourth category, comprising Buildings B, and D, the plug loads encompass sockets, lighting, and split ACs. The contributing factors include historical electricity consumption, indoor $CO_2$ concentration, solar radiation intensity, indoor air temperature, indoor air humidity, and outdoor air temperature.

Overall, in alignment with recent studies and Figure 8, certain influencing factors emerge as significant. First, historical electricity consumption and indoor $CO_2$ concentration, indicative of historical plug-load

energy-use behavior and the number of occupants from the previous hour, significantly impact plug-load electricity consumption. Second, split AC electricity consumption is influenced by indoor and outdoor air temperature, as well as indoor air relative humidity. Finally, lighting electricity consumption is influenced by solar radiation intensity.

### 3.1.2 Results on plug-load electricity consumption prediction

When using the conventional input system, the electricity prediction results with different algorithms are shown in Table 3 as follows.

**Table 3** Contrast experiment results in different buildings using conventional inputs

| Code | Inputs | Algorithms | R | MAPE | RMSE | CV-RMSE | MAE | Times |
|---|---|---|---|---|---|---|---|---|
| A-a’ | Conventional inputs | LSTM | 0.64623 | 16.3942% | 14.4269 | 0.2018 | 10.4338 | 275.019 |
| A-b’ | Conventional inputs | LSTM-WO | 0.7452 | 11.8700% | 12.7318 | 0.1781 | 8.5694 | 893.28 |
| A-c’ | Conventional inputs | Bi-LSTM | 0.70184 | 13.1965% | 13.2445 | 0.1853 | 8.849 | 358.945 |
| A-d’ | Conventional inputs | Bi-LSTM-WO | 0.7452 | 11.8700% | 12.7318 | 0.1781 | 8.5694 | 1069.27 |
| B-a’ | Conventional inputs | LSTM | 0.9093 | 5.9300% | 10.4841 | 0.0890 | 6.515 | 211.059 |
| B-b’ | Conventional inputs | LSTM-WO | 0.9117 | 5.8800% | 10.3485 | 0.0879 | 6.4801 | 560.463 |
| B-c’ | Conventional inputs | Bi-LSTM | 0.93795 | 5.6001% | 8.4974 | 0.0722 | 6.1422 | 243.958 |
| B-d’ | Conventional inputs | Bi-LSTM-WO | 0.94117 | 5.0305% | 8.2738 | 0.0703 | 5.8614 | 785.446 |
| C-a’ | Conventional inputs | LSTM | 0.90644 | 18.3801% | 14.8389 | 0.1462 | 11.4252 | 189.356 |
| C-b’ | Conventional inputs | LSTM-WO | 0.9029 | 16.3900% | 15.0017 | 0.1478 | 10.3571 | 559.2 |
| C-c’ | Conventional inputs | Bi-LSTM | 0.9113 | 16.2800% | 14.3651 | 0.1415 | 10.3037 | 229.675 |
| C-d’ | Conventional inputs | Bi-LSTM-WO | 0.91359 | 14.4122% | 14.2604 | 0.1405 | 10.202 | 722.31 |
| D-a’ | Conventional inputs | LSTM | 0.8802 | 14.4800% | 35.2097 | 0.1362 | 24.805 | 51.627 |
| D-b’ | Conventional inputs | LSTM-WO | 0.8858 | 14.2238% | 33.8772 | 0.1311 | 22.6663 | 137.774 |
| D-c’ | Conventional inputs | Bi-LSTM | 0.8819 | 14.7600% | 34.9173 | 0.1351 | 24.8507 | 60.687 |
| D-d’ | Conventional inputs | Bi-LSTM-WO | 0.89203 | 13.2309% | 32.9397 | 0.1275 | 22.6514 | 163.064 |
| E-a’ | Conventional inputs | LSTM | 0.9479 | 10.1200% | 11.5481 | 0.1306 | 7.2061 | 279.372 |
| E-b’ | Conventional inputs | LSTM-WO | 0.95033 | 9.5296% | 11.3523 | 0.1284 | 7.097 | 814.444 |
| E-c’ | Conventional inputs | Bi-LSTM | 0.9494 | 10.0900% | 11.5056 | 0.1301 | 7.1053 | 325.939 |
| E-d’ | Conventional inputs | Bi-LSTM-WO | 0.9545 | 8.8212% | 10.8659 | 0.1229 | 6.8746 | 982.946 |
| F-a’ | Conventional inputs | LSTM | 0.93406 | 14.4788% | 5.7847 | 0.1524 | 4.283 | 279.923 |
| F-b’ | Conventional inputs | LSTM-WO | 0.9386 | 12.5300% | 5.5311 | 0.1457 | 3.9455 | 853.107 |
| F-c’ | Conventional inputs | Bi-LSTM | 0.9388 | 12.0700% | 5.5167 | 0.1454 | 3.8891 | 329.026 |
| F-d’ | Conventional inputs | Bi-LSTM-WO | 0.95844 | 8.5547% | 4.6065 | 0.1214 | 3.2068 | 995.913 |
| G-a’ | Conventional inputs | LSTM | 0.8599 | 6.9200% | 8.4882 | 0.0898 | 6.4805 | 204.289 |
| G-b’ | Conventional inputs | LSTM-WO | 0.8562 | 6.4686% | 8.47608 | 0.0897 | 6.4686 | 632.87 |
| G-c’ | Conventional inputs | Bi-LSTM | 0.86831 | 6.6379% | 7.9408 | 0.0840 | 6.1565 | 242.301 |
| G-d’ | Conventional inputs | Bi-LSTM-WO | 0.87131 | 6.4461% | 7.8498 | 0.0830 | 6.0166 | 707.999 |

## 3.2 Results on using the novel input system

### 3.2.1 Results on modeling plug-related behavior probabilities

The plug-related behavior probabilities, computed as equation (4), are shown in the following section. The comprehensive results and other information are shown in Tables 4–5 and Figure 9.

**Table 4** Specifications of seven typical buildings

| No. | Types | Opened time in a day | Opened day in a year |
|---|---|---|---|
| A | Office | Opened: All 24 hours | Opened: All 365 days |

| | | | |
|---|---|---|---|
| B | Laboratory | Opened: All 24 hours | Opened: All 365 days |
| C | Library | Opened: 7:00–23:00<br>Closed: 23:00–next 7:00 | Opened: other days<br>Closed: winter vacation |
| D | Library | Opened: 7:00–23:00<br>Closed: 23:00–next 7:00 | Opened: other days<br>Closed: winter vacation |
| E | Teaching building | Opened: 7:00–23:00<br>Closed: 23:00–next 7:00 | Opened: other days (summer, spring, and autumn term)<br>Closed: winter vacation |
| F | Teaching building | Opened: 7:00–23:00<br>Closed: 23:00–next 7:00 | Opened: other days (summer, spring, and autumn term)<br>Closed: winter vacation |
| G | Office | Opened: All 24 hours | Opened: All 365 days |

547 **Table 5** Plug-related energy-use behavior modeling results in seven typical buildings

| No. | Types | Equation results ($x$ is indoor $CO_2$ concentration) |
|---|---|---|
| A | Office | $P_{(T_1\text{-}T_2)} = 0.4658 + \frac{-0.3048}{1+\left(\frac{x}{420.16}\right)^{11.23}}$ |
| B | Laboratory | $P_{(T_1\text{-}T_2)} = 0.6237 + \frac{-0.2291}{1+\left(\frac{x}{417.46156}\right)^{43.96}}$ |
| C | Library | $P_{(T_1\text{-}T_2)} = \begin{cases} 0, \text{ All hours in winter vacation} \\ 0.2, 23{:}00\text{–next } 7{:}00 \text{ in other days} \\ 0.9211 + \frac{-0.4522}{1+\left(\frac{x}{464.83}\right)^{19.49}}, 7{:}00\text{–}23{:}00 \text{ in other days} \end{cases}$ |
| D | Library | $P_{(T_1\text{-}T_2)} = \begin{cases} 0, \text{ All hours in winter vacation} \\ 0.2, 23{:}00\text{–next } 7{:}00 \text{ in other days} \\ 0.7638 + \frac{-0.6122}{1+\left(\frac{x}{521.18}\right)^{7.92}}, 7{:}00\text{–}23{:}00 \text{ in other days} \end{cases}$ |
| E | Teaching building | $P_{(T_1\text{-}T_2)} = \begin{cases} 0, \text{ All hours in winter vacation} \\ 0.05, 23{:}00\text{–next } 7{:}00 \text{ in the whole year except winter vacation} \\ 0.4617 + \frac{-0.0965}{1+\left(\frac{x}{462.97}\right)^{7.00}}, 7{:}00\text{–}23{:}00 \text{ in summer vacation} \\ 247.2973 + \frac{-246.8076}{1+\left(\frac{x}{261036.17}\right)^{1.39}}, 7{:}00\text{–}23{:}00 \text{ in spring term} \\ 0.4407 + \frac{-0.0406}{1+\left(\frac{x}{1111.29}\right)^{12.30}}, 7{:}00\text{–}23{:}00 \text{ in autumn term} \end{cases}$ |
| F | Teaching building | $P_{(T_1\text{-}T_2)} = \begin{cases} 0, \text{ All hours in winter vacation} \\ 0.12, 23{:}00\text{–next } 7{:}00 \text{ in the whole year except winter vacation} \\ 0.4889 + \frac{-0.1790}{1+\left(\frac{x}{450.10}\right)^{28.50}}, 7{:}00\text{–}23{:}00 \text{ in summer vacation} \\ 0.7792 + \frac{-0.3425}{1+\left(\frac{x}{42.25}\right)^{1.98}}, 7{:}00\text{–}23{:}00 \text{ in spring term} \\ 0.7958 + \frac{-0.4014}{1+\left(\frac{x}{498.05}\right)^{4.50}}, 7{:}00\text{–}23{:}00 \text{ in autumn term} \end{cases}$ |
| G | Office | $P_{(T_1\text{-}T_2)} = 0.6809 + \frac{-0.2090}{1+\left(\frac{x}{415.63}\right)^{10.34}}$ |

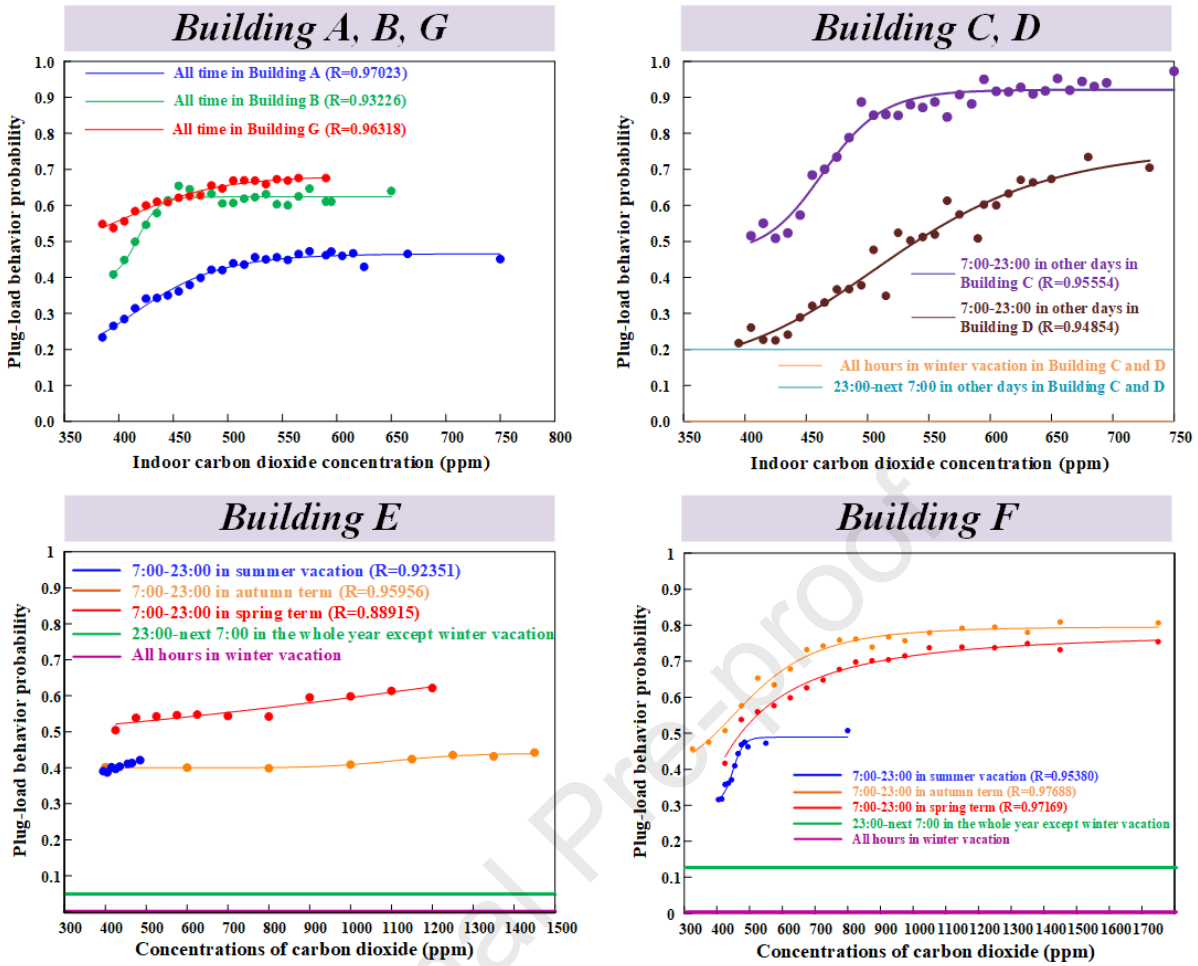


**Figure 9** The result on plug-related behavior probability in different buildings (Note: Due to more cases and insufficient common colors, some colors are reused. Please refer to the legend of each figure for details)

### 3.2.2 Results on plug load electricity consumption prediction

When using the novel input system, the electricity prediction results with different algorithms are shown in Table 6 as follows.

**Table 6** Contrast experiment results in different buildings using novel inputs

| Code | Inputs | Algorithms | R | MAPE | RMSE | CV-RMSE | Times | MAE |
|---|---|---|---|---|---|---|---|---|
| A-a | Novel inputs | LSTM | 0.62654 | 18.0251% | 14.9875 | 0.2097 | 11.3011 | 259.419 |
| A-b | Novel inputs | LSTM-WO | 0.7961 | 12.2500% | 14.8627 | 0.2079 | 10.6002 | 354.547 |
| A-c | Novel inputs | Bi-LSTM | 0.70551 | 13.7911% | 14.5961 | 0.2042 | 10.617 | 329.028 |
| A-d | Novel inputs | Bi-LSTM-WO | 0.8011 | 12.0800% | 12.9612 | 0.1813 | 9.4309 | 1000.311 |
| B-a | Novel inputs | LSTM | 0.92492 | 5.5364% | 9.3796 | 0.0796 | 6.3311 | 193.199 |
| B-b | Novel inputs | LSTM-WO | 0.9307 | 5.8700% | 9.0459 | 0.0768 | 6.3116 | 444.814 |
| B-c | Novel inputs | Bi-LSTM | 0.92949 | 5.4147% | 9.0581 | 0.0769 | 6.1067 | 243.214 |
| B-d | Novel inputs | Bi-LSTM-WO | 0.9302 | 5.6000% | 9.0054 | 0.0765 | 6.1642 | 783.661 |
| C-a | Novel inputs | LSTM | 0.83779 | 16.6535% | 29.2298 | 0.2880 | 17.4981 | 143.39 |
| C-b | Novel inputs | LSTM-WO | 0.953 | 11.5600% | 17.4494 | 0.1719 | 13.9794 | 510.87 |
| C-c | Novel inputs | Bi-LSTM | 0.91942 | 14.3155% | 22.7862 | 0.2245 | 15.0235 | 221.773 |
| C-d | Novel inputs | Bi-LSTM-WO | 0.989 | 11.2200% | 16.9025 | 0.1665 | 13.4734 | 589.506 |
| D-a | Novel inputs | LSTM | 0.88638 | 13.3474% | 54.9682 | 0.2127 | 36.2309 | 40.789 |

| | | | | | | | | |
|---|---|---|---|---|---|---|---|---|
| D-b | Novel inputs | LSTM-WO | 0.9183 | 15.9000% | 49.85178 | 0.1929 | 34.8323 | 129.471 |
| D-c | Novel inputs | Bi-LSTM | 0.90962 | 13.6208% | 52.4021 | 0.2028 | 33.4396 | 54.378 |
| D-d | Novel inputs | Bi-LSTM-WO | 0.9214 | 14.7400% | 48.6128 | 0.1881 | 33.363 | 151.746 |
| E-a | Novel inputs | LSTM | 0.9474 | 10.8800% | 10.4068 | 0.1177 | 6.8604 | 262.682 |
| E-b | Novel inputs | LSTM-WO | 0.9582 | 9.9900% | 10.3087 | 0.1166 | 6.8461 | 744.67 |
| E-c | Novel inputs | Bi-LSTM | 0.94885 | 9.9350% | 11.2671 | 0.1274 | 7.1085 | 323.29 |
| E-d | Novel inputs | Bi-LSTM-WO | 0.96733 | 8.7367% | 10.5939 | 0.1198 | 6.8338 | 917.748 |
| F-a | Novel inputs | LSTM | 0.9034 | 19.8000% | 8.7094 | 0.2295 | 5.4931 | 146.669 |
| F-b | Novel inputs | LSTM-WO | 0.93338 | 14.8898% | 6.6825 | 0.1761 | 4.0531 | 342.684 |
| F-c | Novel inputs | Bi-LSTM | 0.95118 | 13.7072% | 5.7209 | 0.1507 | 3.6806 | 174.727 |
| F-d | Novel inputs | Bi-LSTM-WO | 0.95118 | 13.7072% | 5.7209 | 0.1507 | 3.6806 | 344.336 |
| G-a | Novel inputs | LSTM | 0.82429 | 7.2377% | 8.9969 | 0.0952 | 6.7578 | 195.311 |
| G-b | Novel inputs | LSTM-WO | 0.8694 | 6.6200% | 7.9757 | 0.0844 | 6.106 | 571.928 |
| G-c | Novel inputs | Bi-LSTM | 0.85789 | 6.6997% | 8.0967 | 0.0857 | 6.2744 | 222.627 |
| G-d | Novel inputs | Bi-LSTM-WO | 0.8738 | 6.4800% | 7.8731 | 0.0833 | 6.0672 | 595.09 |

## 4 Discussion

### 4.1 Comparative analyses of the different prediction systems

The focus of this section is on two kinds of energy consumption prediction systems:

(1) Traditional prediction system: It employs conventional inputs and LSTM.

(2) The upgraded prediction system: It uses Bi-LSTM, LSTM-WO, and Bi-LSTM-WO as algorithms in different scenes. For discussing the performance changes, this study defines the prediction system using Bi-LSTM-WO with the conventional input system as the upgraded system (a), and the system using Bi-LSTM-WO with the novel input system as the upgraded system (b).

This investigation exemplifies the above comparison of different prediction systems with illustrated details from Building E as shown in Figure 10. Because the related datasets in Building E are the most complete, while other building energy monitors have missing data. This phenomenon has been also observed in previous studies [39–40]. Although the absence of some data points may not significantly affect the prediction methods, Building E provides a clearer comparison of different prediction systems. Moreover, Building E exhibited complex changes in energy consumption and occupant energy-use behaviors, which allows for a stronger representation of Building E. The comparison of the traditional system and upgraded system (a) is shown in Figure 10. More specifically, the upgraded prediction system displayed elevated prediction performance, vividly captured in Figures 10 and 11.

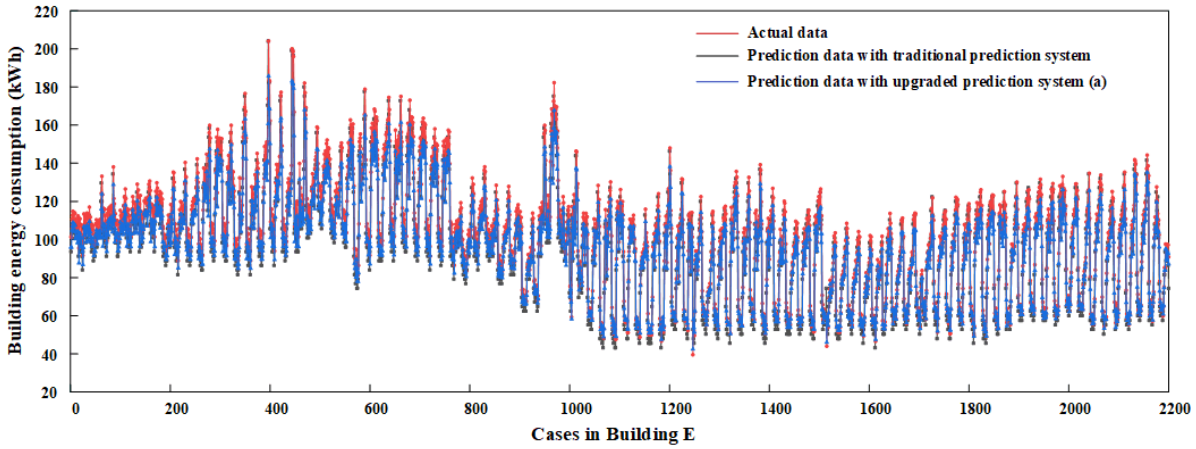


**Figure 10** The comparison of the traditional system and upgraded system (a)

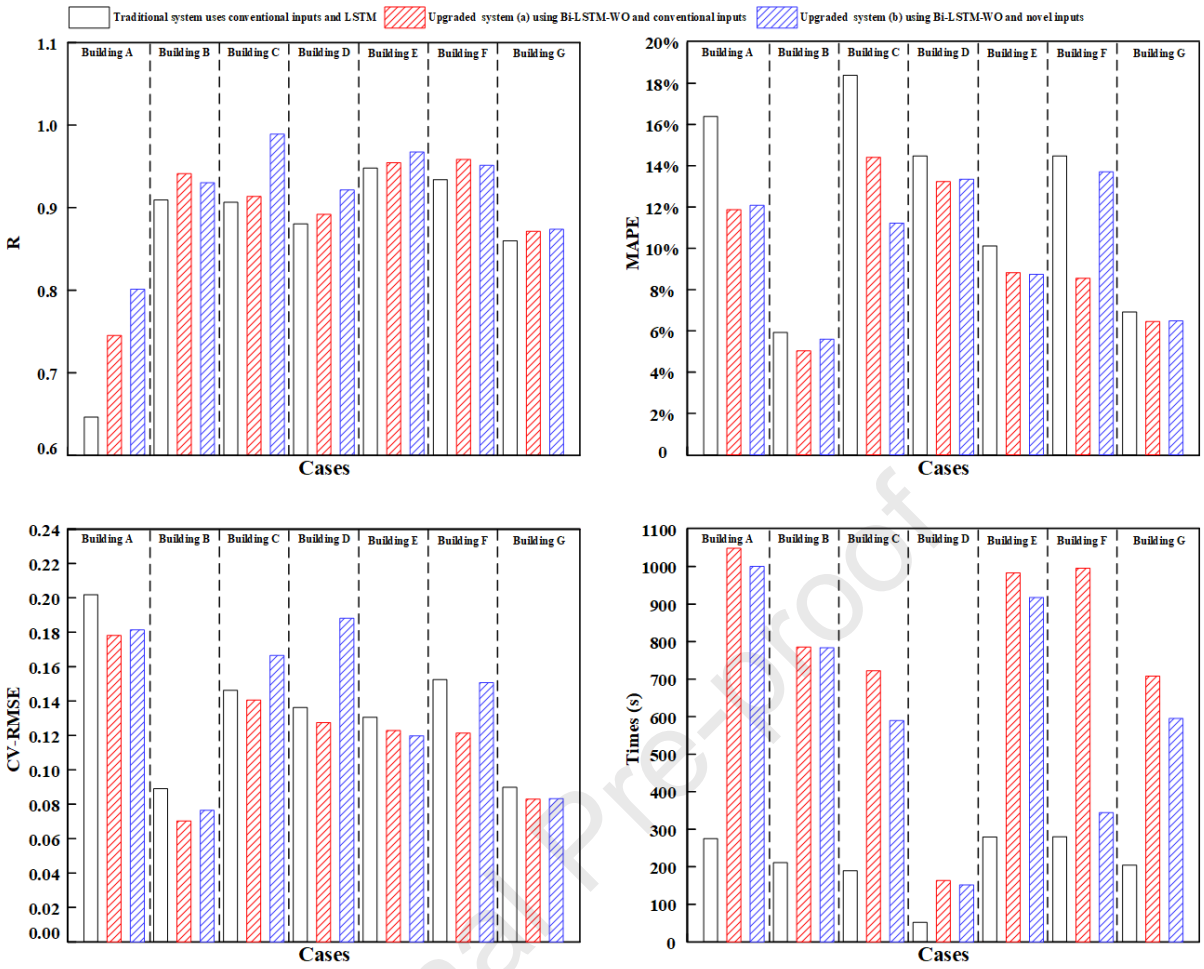


**Figure 11** The comprehensive comparison of the traditional and upgraded prediction system

In a broad comparison, the upgraded system (including a and b) surpasses the traditional prediction system across all building scenarios in terms of fitting, precision, and dispersion performance, while it is accompanied by increased computation time. Without considering outliers (two exceptions): data suggests an increase in fitting performance (R) of 0.0066–0.1549 (range: 0.70%–23.97%), a decrease in precision performance (MAPE) of 0.33%–7.16% (range: 5.33%–40.92%), a decrease in dispersion performance (RMSE) of 0.0638–2.2700 (range: 1.10%–21.08%), a decrease in dispersion performance (CV-RMSE) of 0.0017–0.0310 (range: 1.10%–21.08%), and an increase in time consumption of 64.4130–794.2510 seconds (range 23.01%–288.80%).

### 4.2 Comparative analyses of using different inputs and algorithms

The section delves into the disparity in prediction performance resulting from using different input features and algorithms. Figure 12 reflects the performance improvement or degradation. The red segments coded 1 in Figure 12 are indicative of the scenario where using the novel input system, WO as optimization, and Bi as optimization corresponds to performance improvement demonstrated by decreased elapsed time, MAPE, and CV-RMSE along with increased R. Conversely, prediction performance declines are symbolized by the white segments coded 0. A comparative analysis has been framed to assess the impact of changing the input systems, using Bi, and using WO respectively with other variables remaining constant. It is essential to note that this comparison is quantitative detailing improvements or declines in prediction performance, not offering a qualitative contrast regarding specific values.

**Using novel inputs replacing conventional inputs**

| Building | Algorithms | Comparison term | R | MAPE | CV-RMSE | Times |
|---|---|---|---|---|---|---|
| A | LSTM | Conventional / Novel inputs | 0 | 0 | 0 | 1 |
| A | LSTM-WO | Conventional / Novel inputs | 1 | 0 | 0 | 1 |
| A | Bi-LSTM | Conventional / Novel inputs | 1 | 0 | 0 | 1 |
| A | Bi-LSTM-WO | Conventional / Novel inputs | 1 | 0 | 0 | 1 |
| B | LSTM | Conventional / Novel inputs | 1 | 1 | 1 | 1 |
| B | LSTM-WO | Conventional / Novel inputs | 1 | 1 | 1 | 1 |
| B | Bi-LSTM | Conventional / Novel inputs | 0 | 1 | 0 | 1 |
| B | Bi-LSTM-WO | Conventional / Novel inputs | 0 | 0 | 0 | 1 |
| C | LSTM | Conventional / Novel inputs | 0 | 1 | 0 | 1 |
| C | LSTM-WO | Conventional / Novel inputs | 1 | 1 | 0 | 1 |
| C | Bi-LSTM | Conventional / Novel inputs | 1 | 1 | 0 | 1 |
| C | Bi-LSTM-WO | Conventional / Novel inputs | 1 | 1 | 0 | 1 |
| D | LSTM | Conventional / Novel inputs | 1 | 1 | 0 | 1 |
| D | LSTM-WO | Conventional / Novel inputs | 1 | 0 | 0 | 1 |
| D | Bi-LSTM | Conventional / Novel inputs | 1 | 1 | 0 | 1 |
| D | Bi-LSTM-WO | Conventional / Novel inputs | 1 | 0 | 0 | 1 |
| E | LSTM | Conventional / Novel inputs | 0 | 0 | 1 | 1 |
| E | LSTM-WO | Conventional / Novel inputs | 1 | 0 | 1 | 1 |
| E | Bi-LSTM | Conventional / Novel inputs | 0 | 1 | 1 | 1 |
| E | Bi-LSTM-WO | Conventional / Novel inputs | 1 | 1 | 1 | 1 |
| F | LSTM | Conventional / Novel inputs | 0 | 0 | 0 | 1 |
| F | LSTM-WO | Conventional / Novel inputs | 0 | 0 | 0 | 1 |
| F | Bi-LSTM | Conventional / Novel inputs | 1 | 0 | 0 | 1 |
| F | Bi-LSTM-WO | Conventional / Novel inputs | 0 | 0 | 0 | 1 |
| G | LSTM | Conventional / Novel inputs | 0 | 0 | 0 | 1 |
| G | LSTM-WO | Conventional / Novel inputs | 1 | 0 | 1 | 1 |
| G | Bi-LSTM | Conventional / Novel inputs | 0 | 0 | 0 | 1 |
| G | Bi-LSTM-WO | Conventional / Novel inputs | 1 | 0 | 0 | 1 |

**Using WO as the optimization or not**

| Building | Input | Comparison term | R | MAPE | CV-RMSE | Times |
|---|---|---|---|---|---|---|
| A | Conventional | LSTM / LSTM-WO | 1 | 1 | 1 | 0 |
| A | Conventional | Bi-LSTM / Bi-LSTM-WO | 1 | 1 | 1 | 0 |
| A | Novel | LSTM / LSTM-WO | 1 | 1 | 1 | 0 |
| A | Novel | Bi-LSTM / Bi-LSTM-WO | 1 | 1 | 1 | 0 |
| B | Conventional | LSTM / LSTM-WO | 1 | 1 | 1 | 0 |
| B | Conventional | Bi-LSTM / Bi-LSTM-WO | 1 | 1 | 1 | 0 |
| B | Novel | LSTM / LSTM-WO | 1 | 0 | 1 | 0 |
| B | Novel | Bi-LSTM / Bi-LSTM-WO | 1 | 0 | 1 | 0 |
| C | Conventional | LSTM / LSTM-WO | 0 | 1 | 0 | 0 |
| C | Conventional | Bi-LSTM / Bi-LSTM-WO | 1 | 1 | 1 | 0 |
| C | Novel | LSTM / LSTM-WO | 1 | 1 | 1 | 0 |
| C | Novel | Bi-LSTM / Bi-LSTM-WO | 1 | 1 | 1 | 0 |
| D | Conventional | LSTM / LSTM-WO | 1 | 1 | 1 | 0 |
| D | Conventional | Bi-LSTM / Bi-LSTM-WO | 1 | 1 | 1 | 0 |
| D | Novel | LSTM / LSTM-WO | 1 | 0 | 1 | 0 |
| D | Novel | Bi-LSTM / Bi-LSTM-WO | 1 | 0 | 1 | 0 |
| E | Conventional | LSTM / LSTM-WO | 1 | 1 | 1 | 0 |
| E | Conventional | Bi-LSTM / Bi-LSTM-WO | 1 | 1 | 1 | 0 |
| E | Novel | LSTM / LSTM-WO | 1 | 1 | 1 | 0 |
| E | Novel | Bi-LSTM / Bi-LSTM-WO | 1 | 1 | 1 | 0 |
| F | Conventional | LSTM / LSTM-WO | 1 | 1 | 1 | 0 |
| F | Conventional | Bi-LSTM / Bi-LSTM-WO | 1 | 1 | 1 | 0 |
| F | Novel | LSTM / LSTM-WO | 1 | 1 | 1 | 0 |
| F | Novel | Bi-LSTM / Bi-LSTM-WO | 1 | 1 | 1 | 0 |
| G | Conventional | LSTM / LSTM-WO | 0 | 1 | 1 | 0 |
| G | Conventional | Bi-LSTM / Bi-LSTM-WO | 1 | 1 | 1 | 0 |
| G | Novel | LSTM / LSTM-WO | 1 | 1 | 1 | 0 |
| G | Novel | Bi-LSTM / Bi-LSTM-WO | 1 | 1 | 1 | 0 |

**Using Bi as the optimization or not**

| Building | Input | Comparison term | R | MAPE | CV-RMSE | Times |
|---|---|---|---|---|---|---|
| A | Conventional | LSTM / Bi-LSTM | 1 | 1 | 1 | 0 |
| A | Conventional | LSTM-WO / Bi-LSTM-WO | 1 | 1 | 1 | 0 |
| A | Novel | LSTM / Bi-LSTM | 1 | 1 | 1 | 0 |
| A | Novel | LSTM-WO / Bi-LSTM-WO | 1 | 1 | 1 | 0 |
| B | Conventional | LSTM / Bi-LSTM | 1 | 1 | 1 | 0 |
| B | Conventional | LSTM-WO / Bi-LSTM-WO | 1 | 1 | 1 | 0 |
| B | Novel | LSTM / Bi-LSTM | 1 | 1 | 1 | 0 |
| B | Novel | LSTM-WO / Bi-LSTM-WO | 0 | 1 | 1 | 0 |
| C | Conventional | LSTM / Bi-LSTM | 1 | 1 | 1 | 0 |
| C | Conventional | LSTM-WO / Bi-LSTM-WO | 1 | 1 | 1 | 0 |
| C | Novel | LSTM / Bi-LSTM | 1 | 1 | 1 | 0 |
| C | Novel | LSTM-WO / Bi-LSTM-WO | 1 | 1 | 1 | 0 |
| D | Conventional | LSTM / Bi-LSTM | 1 | 0 | 1 | 0 |
| D | Conventional | LSTM-WO / Bi-LSTM-WO | 1 | 1 | 1 | 0 |
| D | Novel | LSTM / Bi-LSTM | 1 | 0 | 1 | 0 |
| D | Novel | LSTM-WO / Bi-LSTM-WO | 1 | 1 | 1 | 0 |
| E | Conventional | LSTM / Bi-LSTM | 1 | 1 | 1 | 0 |
| E | Conventional | LSTM-WO / Bi-LSTM-WO | 1 | 1 | 1 | 0 |
| E | Novel | LSTM / Bi-LSTM | 1 | 1 | 0 | 0 |
| E | Novel | LSTM-WO / Bi-LSTM-WO | 1 | 1 | 0 | 0 |
| F | Conventional | LSTM / Bi-LSTM | 1 | 1 | 1 | 0 |
| F | Conventional | LSTM-WO / Bi-LSTM-WO | 1 | 1 | 1 | 0 |
| F | Novel | LSTM / Bi-LSTM | 1 | 1 | 1 | 0 |
| F | Novel | LSTM-WO / Bi-LSTM-WO | 1 | 1 | 1 | 0 |
| G | Conventional | LSTM / Bi-LSTM | 1 | 1 | 1 | 0 |
| G | Conventional | LSTM-WO / Bi-LSTM-WO | 1 | 1 | 1 | 0 |
| G | Novel | LSTM / Bi-LSTM | 1 | 1 | 1 | 0 |
| G | Novel | LSTM-WO / Bi-LSTM-WO | 1 | 1 | 1 | 0 |

**Figure 12** Prediction performance improvement and degradation from using different input systems and using optimization algorithms

Overall, the following can be inferred:

First, swapping the conventional input system with the novel system could potentially worsen precision and dispersion performance, as evidenced by a 3.63% average increase in MAPE and a 17.65% average increase in CV-RMSE. However, there was a corresponding decline in calculation time by approximately 17.48%. Despite a diminishment in the overall prediction performance, there were sporadic instances of performance improvement, primarily in buildings B, C, D, and E. These buildings, with complex energy-use behaviors and multiple factors influencing plug-load energy consumption and usage, may explain the lower performance of the traditional prediction system.

Second, the application of WO as optimization predominantly improves the precision and dispersion performance, documented by a 10.96% average decrease in MAPE and a 7.19% average decrease in CV-RMSE. However, the calculation time increases substantially by an average of 183.14%. The elongated duration could be attributed to the requirement of additional iterations by the WO to pinpoint an optimal hyperparameter solution.

Finally, the application of Bi as optimization was similar to those using WO as optimization. Despite accruing a similar accuracy improvement with an average decrease of 9.66% in MAPE and 7.12% in CV-RMSE, the increase in operation time consumption was relatively marginal, recorded at an average increase of 28.93%. This may mean a greater balance of using Bi as optimization in comparison with WO.

### 4.3 Applicability and propensity

The performance and suitability of using different input features and algorithms vary across scenarios. A set of guiding principles to assist in these variations is presented herein and elaborated in Figure 13.

(1) Considering input selection, three main principles have been established as follows:

First, the capacity for data collection varies. In the absence of access to outdoor meteorological parameters or determining the category of plug-loads, the novel input system becomes the only feasible option. By contrast, the conventional input system remains a viable selection when there is a lack of duration time data for plug-load usages. And if all kinds of data can be collected, the propensity may be influenced by other principles and using which algorithms.

Second, in buildings exhibiting a multitude of factors influencing plug-load electricity consumption or relatively complex energy-use behavior such as Buildings B–E, the novel and conventional input systems exhibit comparable performance. Both these systems present distinct advantages and disadvantages. However, in predicting energy consumption in buildings with simpler changes in energy consumption and occupant behaviors, the conventional input system shows better performance.

Finally, the novel input system proves more effective under time constraints.

(2) Considering algorithm selection, two main principles have been established as follows:

First, in situations where accuracy is paramount, the use of WO or Bi for optimization is recommended. Finally, WO for optimization may be not suitable for scenarios with strict time constraints.

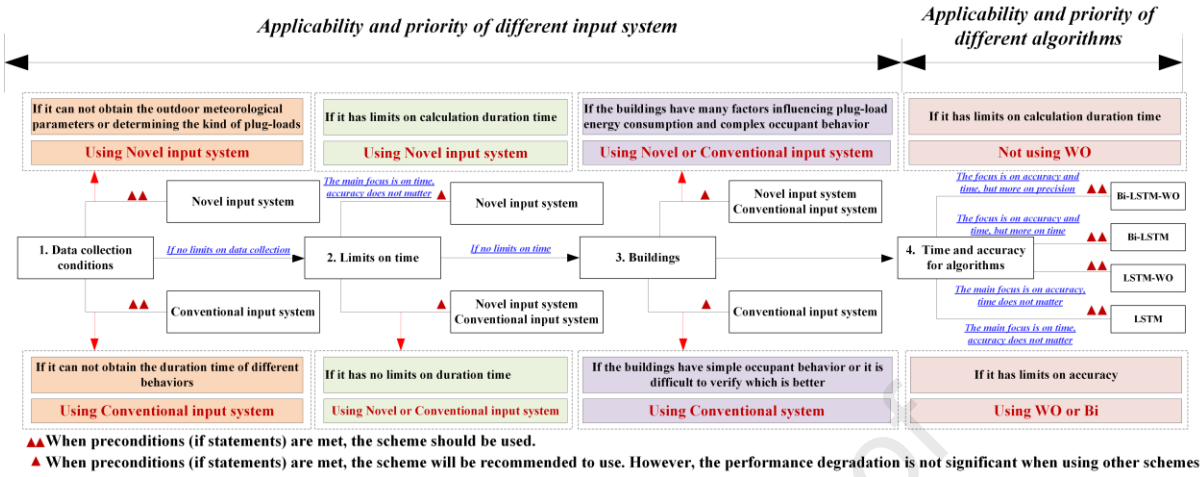


**Figure 13** The applicability and priority of different input systems and algorithms

Following the principles and Figure 13, a comprehensive plug-load electricity consumption prediction method has been proposed. This comprehensive method comprises two input systems and four algorithms, intended not to eradicate traditional inputs or algorithms, instead, it complements them to overcome challenges associated with the traditional prediction system such as data collection difficulty and poor prediction accuracy.

### 4.4 Limits

(1) There may be a need for more kinds of buildings to be included in the study in the future.

(2) For the conventional input system, identifying various categories of plug loads poses a significant challenge. This complexity arises when different rooms in a building incorporate different categories of plug loads. For example, the plug loads in Room 1 may include sockets, lighting, and split ACs, whereas the plug load in Room 2 may only include sockets and lighting. As such, pinpointing the categories of plug loads across an entire building may be a challenge, making it a noteworthy area for further exploration.

(3) For the novel input system, the modeling of socket-related behavior especially random socket-related behaviors still requires further development. Notably, indoor air temperature and illumination can mainly determine AC and lighting-related behaviors respectively. In contrast, the $CO_2$ concentration only indirectly reflects the probability of socket-related behaviors through the number of occupants. This indirect relationship could potentially be compromised, especially if there is frequent variability in occupant behavior patterns or the number of occupants. Furthermore, certain sockets are interconnected with lighting and split ACs, most prominently in spaces such as single-person offices or residences. Moreover, conventional modeling methods centered around waiting times and questionnaires fail to provide accurate, real-time, and online data. Thus, it is crucial to address the pressing need for the continued development of socket-related behavior modeling methods. Referring to recent studies, a hybrid model of stochastic Markov models with $CO_2$-based statistical models may serve to further enhance the probabilistic model of socket-related behaviors.

## 5 Conclusion

This study presents a comprehensive upgraded plug-load electricity consumption prediction system, employing Bi-LSTM as a base algorithm in place of LSTM and employing improved WO for optimization. Moreover, it proposes two input systems for facing different limits and conditions on data collection, time requirements, and accuracy requirements. One is the conventional input system depending on factors

affecting electricity consumption, and the other is the novel input system introducing probabilities of socket-related behaviors based on the conventional input system. Key findings include:

(1) Comparison of the different building energy consumption prediction systems: the upgraded system deploying Bi-LSTM-WO demonstrated a better fitting (R increased by 0.70%–23.97%), precision (MAPE decreased by 5.33%–40.92%), and dispersion performance (CV-RMSE decreased by 1.10%–21.08%), while it needs longer computation time (Time increased by 23.01%–288.80%), except in isolated cases. Comparing the averages of indices, the upgraded system using Bi-LSTM-WO has 5.08% of R increase, 16.97% of MAPE decrease, and 4.71% of CV-RMSE decrease with 228.25% of time increase; using Bi-LSTM has 2.29% of R increase, 8.47% of MAPE decrease, -2.80% of CV-RMSE decrease with 13.01% of time increase; and using LSTM-WO has 3.80% of R increase, 9.37% of MAPE decrease, -1.81% of CV-RMSE decrease with 156.27% of time increase. Therefore, the most suitable selection of prediction schemes should weigh time and accuracy constraints.

(2) Comparison of different input systems: the conventional input system necessitates building plug load classification, and factors affecting the electricity consumption for each category, whereas the novel input system requires probabilities of socket-related behaviors. The latter, despite showing a slightly inferior precision and dispersion performance (MAPE increased by 3.63% and CV-RMSE increased by 17.65%), outperforms in terms of reducing calculation time consumption (Times decreased by 17.48%). Moreover, it is worth noting that the data reveals the better performance of the novel input system in some special buildings with more factors influencing plug-load energy consumption and relatively complex energy-use behaviors.

(3) Applicability and propensity of different input systems: the selection between the two input systems depends primarily on data collection conditions, building type, and time limitations. First, concerning data collection conditions, the conventional input system requires more sensors to obtain parameters and more consultation to determine the categories of building plug loads. Moreover, it needs to further analyze the suitable category for the whole building when the categories of plug loads are different in each room. Novel input needs the time duration of occupant behaviors for calculating the probability. Second, concerning building type, the novel input system may be more suitable in buildings with complex energy-use behaviors and factors influencing plug-load energy consumption, while the conventional input system is relatively universally applicable. Finally, concerning time consumption, if it has limits on calculation time, the novel input system may be better.

(4) Comparison of different algorithms: WO with adaptive weight adjustment and chaotic mapping presents a viable path toward the optimal solution of hyperparameters. Concurrently Bi exhibits the capacity to assimilate both historical and future states which affect the current state. Therefore, using WO and Bi as optimization will improve the performance, theoretically. Experimental data substantiate these presumptions. Using WO improves the precision and dispersion performance (MAPE decreased by 10.96% and CV-RMSE decreased by 7.19%) with increasing the calculation time (Times increased by 183.14%). However, using Bi will result in a similar accuracy improvement (MAPE decreased by 9.66% and CV-RMSE decreased by 7.12%) with relatively less increase in calculation time consumption (Times increased by 28.93%).

(5) Applicability and propensity of different algorithms: Considering constraints in precision, using WO or Bi or Both these two optimizations may be necessary. Overall, WO will improve the fitting, precision, and dispersion performance more than Bi, but the difference is insignificant. By contrast, WO will need more time than Bi and the difference is significant. Therefore, if it has strict limits on calculation time, using WO may be not suitable. Therefore, in the broader perspective that factors in calculation time consumption, algorithm complexity, and performance improvement, Bi often demonstrates more applications to WO as

optimization in most cases.

**Acknowledgment**

The work described in this paper was supported by the National Natural Science Foundation of China (Grant No. 52078096), the Fundamental Research Funds for the Central Universities (Grant No. DUT20JC47), and the Technology Development Funds for PCI Technology Group (Grant No. 2111CGZB0011/1000010164).

**References**

[1] A Streltsov, J M Malof, B Huang, K Bradbury. Estimating residential building energy consumption using overhead imagery. Applied Energy, 2020, 280, 116018. https://doi.org/10.1016/j.apenergy.2020.116018

[2] X Cao, X Dai, J Liu. Building energy-consumption status worldwide and the state-of-the-art technologies for zero-energy buildings during the past decade. Energy and Buildings, 2016, 128, 198-213. https://doi.org/10.1016/j.enbuild.2016.06.089

[3] China Association of Building Energy Efficiency. 2022 China Urban and Rural Construction Carbon Emission Series Research Report. 2023.01.04. In Chinese. From: https://www.cabee.org/site/content/24420.html

[4] Li L, Zhang S. Techno-economic and environmental assessment of multiple distributed energy systems coordination under centralized and decentralized framework. Sustainable Cities and Society, 2021, 72, 103076. https://doi.org/10.1016/j.scs.2021.103076

[5] Qi S, Zhou C, Li K et al. The impact of a carbon trading pilot policy on the low-carbon international competitiveness of industry in China: An empirical analysis based on a DDD model. Journal of Cleaner Production, 2021, 281, 125361. https://doi.org/10.1016/j.jclepro.2020.125361

[6] Jiang H, Jiang P, Wang Det al. Can smart city construction facilitate green total factor productivity? A quasi-natural experiment based on China's pilot smart city. Sustainable Cities and Society, 2021, 69, 102809. https://doi.org/10.1016/j.scs.2021.102809

[7] Maltais, L., & Gosselin, L. Forecasting of short-term lighting and plug load electricity consumption in single residential units: Development and assessment of data-driven models for different horizons. Applied Energy. 2022, 307, 118229. https://doi.org/10.1016/j.apenergy.2021.118229

[8] Jenkins, C., Young, R., Tsau, J., Razavi, H., Kaplan, J., & Ibeziako, M.O. Effective management of plug loads in commercial buildings with occupant engagement and centralized controls. Energy and Buildings. 2019, 201, 194-201. https://doi.org/10.1016/j.enbuild.2019.06.030

[9] Christiansen, N., Kaltschmitt, M., Dzukowski, F., & Isensee, F. Electricity consumption of medical plug loads in hospital laboratories: Identification, evaluation, prediction and verification. Energy and Buildings. 2015, 107, 392-406. https://doi.org/10.1016/j.enbuild.2015.08.022

[10] Anand, P., Cheong, D., Sekhar, C., Santamouris, M., & Kondepudi, S. Energy saving estimation for plug and lighting load using occupancy analysis. Renewable Energy. 2019, 143, 1143-1161. https://doi.org/10.1016/j.renene.2019.05.089

[11] Jensen, S.Ø., Marszal-Pomianowska, A., Lollini, R., Pasut, W., Knotzer, A., & Engelmann, P., et al. IEA EBC Annex 67 Energy Flexible Buildings. Energy and Buildings. 2017, 155, 25-34. https://doi.org/10.1016/j.enbuild.2017.08.044

[12] Jia, C., Zhang, L., Zhang, C., & Li, Y. Intelligent decision optimization for energy control of direct current power distribution system with multi-port access for intelligent buildings. Alexandria Engineering Journal. 2023, 63, 455-464. https://doi.org/10.1016/j.aej.2022.08.007

[13] Castillo-Calzadilla, T., Macarulla, A.M., Kamara-Esteban, O., & Borges, C.E. A case study comparison between photovoltaic and fossil generation based on direct current hybrid microgrids to power a service building. 2020, Journal of Cleaner Production. 244, 118870. https://doi.org/10.1016/j.jclepro.2019.118870

[14] Tang, H., & Wang, S. Life-cycle economic analysis of thermal energy storage, new and second-life batteries in buildings for providing multiple flexibility services in electricity markets. Energy. 2023, 264, 126270.

https://doi.org/10.1016/j.energy.2022.126270
[15] Shen, M., & Chen, J. Optimization of peak-valley pricing policy based on a residential electricity demand model. Journal of Cleaner Production. 2022, 380, 134761. https://doi.org/10.1016/j.jclepro.2022.134761
[16] M K Kim, Y Kim, J Srebric. Impact of correlation of plug load data, occupancy rates and local weather conditions on electricity consumption in a building using four back-propagation neural network models. Sustainable Cities and Society, 2020, 62, 102321. https://doi.org/10.1016/j.scs.2020.102321
[17] S Clemente, S Beauchêne, E Nefzaoui. Generation of aggregated plug load profiles in office buildings. Energy and Buildings, 2021, 252, 111398. https://doi.org/10.1016/j.enbuild.2021.111398
[18] A C Menezes, A Cripps, R A Buswell, D Bouchlaghem. Benchmarking small power energy consumption in office buildings in the United Kingdom: A review of data published in CIBSE Guide F. Building Services Engineering Research and Technology, 2012, 34(1), 73-86. https://doi.org/10.1177/0143624412465092
[19] P Anand, D Cheong, C Sekhar, M Santamouris, S Kondepudi. Energy saving estimation for plug and lighting load using occupancy analysis. Renewable Energy, 2019, 143, 1143-1161. https://doi.org/10.1016/j.renene.2019.05.089
[20] A Mahdavi, F Tahmasebi, M Kayalar. Prediction of plug loads in office buildings: Simplified and probabilistic methods. Energy and Buildings, 2016, 129, 322-329. https://doi.org/10.1016/j.enbuild.2016.08.022
[21] P Gandhi, G S Brager. Commercial office plug load energy consumption trends and the role of occupant behavior. Energy and Buildings, 2016, 125, 1-8. https://doi.org/10.1016/j.enbuild.2016.04.057
[22] Chen, S., Wu, J., Pan, Y., Ge, J., & Huang, Z. Simulation and case study on residential stochastic energy use behaviors based on human dynamics. *Energy and Buildings*. 2020, 223, 110182. https://doi.org/10.1016/j.enbuild.2020.110182
[23] Zhou, X., Mei, Y., Liang, L., Mo, H., Yan, J., & Pan, D. Modeling of occupant energy consumption behavior based on human dynamics theory: A case study of a government office building. *Journal of Building Engineering*. 2022, 58, 104983. https://doi.org/10.1016/j.jobe.2022.104983
[24] A Kamilaris, B Kalluri, S Kondepudi, T Kwok Wai. A literature survey on measuring energy usage for miscellaneous electric loads in offices and commercial buildings. Renewable and Sustainable Energy Reviews, 2014, 34, 536-550. https://doi.org/10.1016/j.rser.2014.03.037
[25] Zhao T, Zhang C, Xu Jet al. Data-driven correlation model between human behavior and energy consumption for college teaching buildings in cold regions of China. Journal of Building Engineering, 2021, 38, 102093. https://doi.org/10.1016/j.jobe.2020.102093
[26] R. Tuttle, K. Trenbath, K. Maisha, A. LeBar. Assessing and Reducing Plug and Process Loads in Office Buildings. Publisher: National Renewable Energy Lab (NREL), Golden, CO (United States). 2020, 1–9. https://digital.library.unt.edu/ark:/67531/metadc843212/
[27] Das, A., Annaqeeb, M.K., Azar, E., Novakovic, V., & Kjærgaard, M.B. Occupant-centric miscellaneous electric loads prediction in buildings using state-of-the-art deep learning methods. Applied Energy,2020, 269, 115135. https://doi.org/10.1016/j.apenergy.2020.115135
[28] R Markovic, E Azar, M K Annaqeeb, J Frisch, C V Treeck. Day-ahead prediction of plug-in loads using a long short-term memory neural network. Energy and Buildings, 2021, 234, 110667. https://doi.org/10.1016/j.enbuild.2020.110667
[29] Cucca, G., & Ianakiev, A. Assessment and optimisation of energy consumption in building communities using an innovative co-simulation tool. *Journal of Building Engineering*. 2020, 32, 101681. https://doi.org/10.1016/j.jobe.2020.101681
[30] Shabunko, V., Lim, C.M., & Mathew, S. EnergyPlus models for the benchmarking of residential buildings in Brunei Darussalam. *Energy and Buildings*. 2018, 169, 507-516. https://doi.org/10.1016/j.enbuild.2016.03.039
[31] Ghofrani, A., Nazemi, S.D., & Jafari, M.A. HVAC load synchronization in smart building communities. *Sustainable Cities and Society*. 2019, 51, 101741. https://doi.org/10.1016/j.scs.2019.101741
[32] Balvedi, B.F., Ghisi, E., & Lamberts, R. A review of occupant behaviour in residential buildings. *Energy and*

*Buildings*. 2018, 174, 495-505. https://doi.org/10.1016/j.enbuild.2018.06.049

[33] H Sha, P Xu, C Yan, Y Ji, K Zhou, F Chen. Development of a key-variable-based parallel HVAC energy predictive model. Building Simulation, 2022, 15(7), 1193-1208. https://doi.org/10.1007/s12273-021-0885-0

[34] S Zhan, G Wichern, C Laughman, A Chong, A Chakrabarty. Calibrating building simulation models using multi-source datasets and meta-learned Bayesian optimization. Energy and Buildings, 2022, 270, 112278. https://doi.org/10.1016/j.enbuild.2022.112278

[35] M. Bourdeau, X. Q. Zhai, E. Nefzaoui, X. Guo and P. Chatellier. Modeling and forecasting building energy consumption: A review of data-driven techniques. *Sustainable Cities and Society*, 2019, 48, 101533. https://doi.org/10.1016/j.scs.2019.101533

[36] Amasyali, K., & El-Gohary, N.M. A review of data-driven building energy consumption prediction studies. *Renewable and Sustainable Energy Reviews*. 2018, 81, 1192-1205. https://doi.org/10.1016/j.rser.2017.04.095

[37] Li, Y., O'Neill, Z., Zhang, L., Chen, J., Im, P., & DeGraw, J. Grey-box modeling and application for building energy simulations-A critical review. Renewable and Sustainable Energy Reviews, 2021, 146, 111174. https://doi.org/10.1016/j.rser.2021.111174

[38] M H Shamsi, U Ali, E Mangina, J O Donnell. Feature assessment frameworks to evaluate reduced-order grey-box building energy models. Applied Energy, 2021, 298, 117174. https://doi.org/10.1016/j.apenergy.2021.117174

[39] Zhao T, Zhang C, Ujeed T, Ma L. Online Methodology for Separating the Power Consumption of Lighting Sockets and Air-Conditioning in Public Buildings Based on an Outdoor Temperature Partition Model and Historical Energy Consumption Data. *Applied Sciences*. 2021, 11(3):1031. https://doi.org/10.3390/app11031031

[40] Yan, H., Ma, L., Zhao, T., & Zhang, J. Research on repair method of abnormal energy consumption data of lighting and plug based on similar features. *Energy and Buildings*. 2022, 268, 112155. https://doi.org/10.1016/j.enbuild.2022.112155

[41] S Mirjalili, A Lewis. The Whale Optimization Algorithm. Advances in Engineering Software, 2016, 95, 51-67. https://doi.org/10.1016/j.advengsoft.2016.01.008

[42] TENG Zhijun, LÜ Jinling, GUO Liwen, XU Yuanyuan. An improved hybrid grey wolf optimization algorithm based on Tent mapping. Journal of Harbin Institute of Technology, 2018, 50(11): 40-49. https://doi.org/10.11918/j.issn.0367-6234.201806096

[43] Y Yu, S Gao, S Cheng, Y Wang, S Song, F Yuan. CBSO: a memetic brain storm optimization with chaotic local search. Memetic Computing, 2018, 10(4), 353-367. https://doi.org/10.1007/s12293-017-0247-0

[44] C Zhang, L Ma, X Han, T Zhao. Improving building energy consumption prediction using occupant-building interaction inputs and improved swarm intelligent algorithms. Journal of Building Engineering, 2023, 73, 106671. https://doi.org/10.1016/j.jobe.2023.106671

[45] D Sheikh Khan, J Kolarik, C Anker Hviid, P Weitzmann. Method for long-term mapping of occupancy patterns in open-plan and single office spaces by using passive-infrared (PIR) sensors mounted below desks. Energy and Buildings. 2021, 230, 110534. https://doi.org/10.1016/j.enbuild.2020.110534

[46] Y R Yoon, Y R Lee, S H Kim, J W Kim, H J Moon. A non-intrusive data-driven model for detailed occupants' activities classification in residential buildings using environmental and energy usage data. Energy and Buildings, 2022, 256, 111699. https://doi.org/10.1016/j.enbuild.2021.111699

[47] H Zhou, J Yu, Y Zhao, C Chang, J Li, B Lin. Recognizing occupant presence status in residential buildings from environment sensing data by data mining approach. Energy and Buildings, 2021, 252, 111432. https://doi.org/10.1016/j.enbuild.2021.111432

[48] P F Pereira, N M M Ramos. Detection of occupant actions in buildings through change point analysis of in-situ measurements. Energy and Buildings, 2018, 173, 365-377. https://doi.org/10.1016/j.enbuild.2018.05.050

[49] China Meteorological Administration. China Meteorological Science Data Center. From: http://data.cma.cn

[50] G Xianliang, X Jingchao, L Zhiwen, L Jiaping. Analysis to energy consumption characteristics and influencing factors of terminal building based on airport operating data. Sustainable Energy Technologies and Assessments, 2021, 44, 101034. https://doi.org/10.1016/j.seta.2021.101034

[51] L Yuan, Y Ruan, G Yang, F Feng, Z Li. Analysis of Factors Influencing the Energy Consumption of Government Office Buildings in Qingdao. Energy Procedia, 2016, 104, 263-268. https://doi.org/10.1016/j.egypro.2016.12.045

[52] A S Weerasinghe, J O B Rotimi, E O Rasheed. Modelling of underlying social psychological effects on occupant energy-related behaviours. Building and Environment, 2023, 231, 110055. https://doi.org/10.1016/j.buildenv.2023.110055

[53] S Carlucci, M De Simone, S K Firth, M B Kjærgaard, R Markovic, M S Rahaman, M K Annaqeeb, S Biandrate, A Das, J W Dziedzic, G Fajilla, M Favero, M Ferrando, J Hahn, M Han, Y Peng, F Salim, A Schlüter, C van Treeck. Modeling occupant behavior in buildings. Building and Environment, 2020, 174, 106768. https://doi.org/10.1016/j.buildenv.2020.106768

[54] X Zhou, D Yan, T Hong, X Ren. Data analysis and stochastic modeling of lighting energy use in large office buildings in China. Energy and Buildings, 2015, 86, 275-287. https://doi.org/10.1016/j.enbuild.2014.09.071

[55] D Yan, W O Brien, T Hong, X Feng, H Burak Gunay, F Tahmasebi, A Mahdavi. Occupant behavior modeling for building performance simulation: Current state and future challenges. Energy and Buildings, 2015, 107, 264-278. https://doi.org/10.1016/j.enbuild.2015.08.032

[56] M Yang, M K Lim, Y Qu, X Li, D Ni. Deep neural networks with L1 and L2 regularization for high dimensional corporate credit risk prediction. Expert Systems with Applications, 2023, 213, 118873. https://doi.org/10.1016/j.eswa.2022.118873

[57] Y Li, S Wang, Q Chen, X Wang. Comparative Study of Several New Swarm Intelligence Optimization Algorithms. Computer Engineering and Applications, 2020, 56(22): 1-12. (In Chinese: http://cea.ceaj.org/CN/Y2020/V56/I22/1)

[58] S Yelisetti, V K Saini, R Kumar, R Lamba, A Saxena. Optimal energy management system for residential buildings considering the time of use price with swarm intelligence algorithms. Journal of Building Engineering, 2022, 59, 105062.

[59] H Zhou, J Yu, Y Zhao, C Chang, J Li, B Lin. Recognizing occupant presence status in residential buildings from environment sensing data by data mining approach. Energy and Buildings, 2021, 252, 111432. https://doi.org/10.1016/j.enbuild.2021.111432 .

[60] D Yan, T Hong, B Dong, A Mahdavi, S D Oca, I Gaetani, X Feng. IEA EBC Annex 66: Definition and simulation of occupant behavior in buildings. Energy and Buildings, 2017, 156, 258-270. https://doi.org/10.1016/j.enbuild.2017.09.084

**Appendix: Demonstration of the program for each part of the proposed prediction algorithm (MATLAB)**

**%% Data pre-processing**

```
%%  Empty the matlab environment
warning off                 % Close alarm messages
close all                   % Close the open chart window
clear                       % Clear variables
clc                         % Clear command line

%%  Importing Data
res = xlsread('data.xlsx');

%%  Data Analysis
num_size = 0.7;                              % Ratio of training set to data set
outdim = 1;                                  % The last column is the output
num_samples = size(res, 1);                  % Number of samples
res = res(randperm(num_samples), :);         % Disrupting the data set
num_train_s = round(num_size * num_samples); % Number of training set samples
f_ = size(res, 2) - outdim;                  % Input Feature Dimension

%%  Dividing the training set and test set
P_train = res(1: num_train_s, 1: f_)';
T_train = res(1: num_train_s, f_ + 1: end)';
M = size(P_train, 2);

P_test = res(num_train_s + 1: end, 1: f_)';
T_test = res(num_train_s + 1: end, f_ + 1: end)';
N = size(P_test, 2);

%%  Data normalization
[p_train, ps_input] = mapminmax(P_train, 0, 1);
p_test = mapminmax('apply', P_test, ps_input);

[t_train, ps_output] = mapminmax(T_train, 0, 1);
t_test = mapminmax('apply', T_test, ps_output);
```

**%% Bi-LSTM-WO**

```
% Set parameters for Whale Optimization Algorithm (WOA)
popsize = 5; % Number of individuals in the population
maxgen = 10; % Maximum number of iterations for WOA
dim = 4; % Number of variables to be optimized, namely the number of nodes in the first and second hidden layers of
BiLSTM, maximum training epochs, and initial learning rate
% Normalization and cell array handling
lb = [1, 1, 0.001]; % Lower bounds for the variables
```

```
ub = [10, 20, 0.01]; % Upper bounds for the variables

% Initialize position vector and score for the leader
Leader_pos = zeros(1, dim);
Leader_score = inf; % Change this to -inf for maximization problems

% Initialize the positions of search agents
Positions = initialization(popsize, dim, ub, lb); % Positions of multiple individuals in the population

Convergence_curve = zeros(1, maxgen); % Convergence curve

t = 1; % Loop counter

% Main loop
while t < maxgen + 1
    disp(['current iteration is: ', num2str(t)]) % Display current iteration

    for i = 1:size(Positions, 1)
        % Return back search agents that go beyond the search space boundaries
        Flag4ub = Positions(i, :) > ub;
        Flag4lb = Positions(i, :) < lb;
        Positions(i, :) = (Positions(i, :) .* (~(Flag4ub + Flag4lb))) + ub .* Flag4ub + lb .* Flag4lb;

        % Evaluate fitness of the individual, which calls the 'func.m' sub-function and assigns the position coordinates to
the parameters of BiLSTM for training
        [fitness, net] = func(Positions(i, :), p_train, P_train, P_test, tn_train, ts, t_train, t_test); % Calculate fitness

        if fitness < Leader_score % Update the leader if better fitness is found
            Leader_score = fitness;
            Leader_pos = Positions(i, :);
            net1 = net;
        end
    end

    a = 2 - t * ((2) / maxgen); % a decreases linearly from 2 to 0
    a2 = -1 + t * ((-1) / maxgen); % a2 linearly decreases from -1 to -2

    % Update the position of search agents
    for i = 1:size(Positions, 1)
        r1 = rand(); % r1 is a random number in [0,1]
        r2 = rand(); % r2 is a random number in [0,1]

        A = 2 * a * r1 - a; % Eq. (8) in the paper
        C = 2 * r2; % Eq. (7) in the paper
```

```
            b = 1;
            l = (a2 - 1) * rand + 1;

            p = rand();

            % Update position for each dimension of the individual
            for j = 1:size(Positions, 2)
                if p < 0.5 % Shrinking encircling mechanism
                    if abs(A) >= 1
                        rand_leader_index = floor(popsize * rand() + 1); % Find a random leader index
                        X_rand = Positions(rand_leader_index, :);
                        D_X_rand = abs(C * X_rand(j) - Positions(i, j));
                        Positions(i, j) = X_rand(j) - A * D_X_rand;
                    elseif abs(A) < 1
                        D_Leader = abs(C * Leader_pos(j) - Positions(i, j));
                        Positions(i, j) = Leader_pos(j) - A * D_Leader;
                    end
                elseif p >= 0.5 % Spiral updating position mechanism
                    distance2Leader = abs(Leader_pos(j) - Positions(i, j));
                    Positions(i, j) = distance2Leader * exp(b * l) * cos(l * 2 * pi) + Leader_pos(j);
                end
            end
        end

        Convergence_curve(t) = Leader_score;
        t = t + 1;

        disp(t)
    end

    figure;
    plot(Convergence_curve, 'b-', 'LineWidth', 1.0)
    grid on
    xlabel('Generation')
    ylabel('Best Fitness')
    title('Convergence Curve for WOA Optimization')

    disp('Optimized BiLSTM Parameters using WOA:')
    disp(strcat('Optimal Parameters: ', num2str([round(Leader_pos(1:2)), Leader_pos(3)])))
    disp(strcat('Best Fitness: ', num2str(Leader_score)))

    %% Assign optimized parameters to BiLSTM neural network after WOA optimization (After the while loop, assign the
    optimized parameters to BiLSTM and train it again)
```

```
% Set parameters
numFeatures = size(p_train, 1); % Number of input layer nodes
numHiddenUnits1 = round(Leader_pos(1)); % Number of nodes in the first hidden layer
numResponses = 1; % Number of nodes in the fully connected layer (equal to the number of labels)

% Create the network
layers = [ ...
    sequenceInputLayer(numFeatures)
    bilstmLayer(numHiddenUnits1, 'OutputMode', 'last', 'name', 'hidden1')
    dropoutLayer(0.2, 'name', 'dropout_1') % Dropout layer to prevent overfitting in the first hidden layer
    fullyConnectedLayer(numResponses, 'name', 'fullconnect')
    regressionLayer('name', 'out')]; % Regression layer

% Set options
options = trainingOptions('adam', ... % Optimization algorithm
    'MaxEpochs', round(Leader_pos(2)), ... % Maximum number of epochs to iterate through the samples
    'GradientThreshold', 1, ... % Gradient threshold
    'InitialLearnRate', Leader_pos(3), ... % Initial learning rate
    'LearnRateSchedule', 'piecewise', ... % Learning rate schedule
    'LearnRateDropPeriod', 800, ... % Learning rate update after 100 epochs
    'LearnRateDropFactor', 0.8, ... % Reduce learning rate by multiplying with this factor 0.1
    'MiniBatchSize', 240, ... % Batch size for processing samples
    'Verbose', 1, ... % Whether to display training progress in the command console
    'Plots', 'training-progress');

% Train BiLSTM
% net = trainNetwork(P_train,tn_train',layers,options);
net = net1;

% Test set prediction
testn_simu = predict(net, P_test);
test_simu = mapminmax('reverse', testn_simu', ts);

disp('WOA-BiLSTM Neural Network Performance Analysis:')
[e, ape] = caculate_perf(t_test, test_simu);

rmse = sqrt(mean((test_simu - t_test).^2));
```

**%% 'Initialization' in previous program ('Bi-LSTM-WO')**

```
%% func.
function [fitness, net] = func(x, p_train, P_train, P_test, tn_train, ts, t_train, t_test)
% Fitness subfunction
% Optimizes the number of nodes in the first and second hidden layer of a BiLSTM network,
```

```
% as well as the maximum training iterations and initial learning rate.
% Parameter settings
numFeatures = size(p_train, 1); % Number of input layer nodes
numHiddenUnits1 = round(x(1)); % Number of nodes in the first hidden layer
numResponses = 1; % Number of nodes in the fully connected layer (equals the number of labels)

%% Create the network
layers = [ ...
    sequenceInputLayer(numFeatures)
    bilstmLayer(numHiddenUnits1, 'OutputMode', 'last', 'name', 'hidden1')
    dropoutLayer(0.3, 'name', 'dropout_1') % Dropout layer to prevent overfitting in hidden layer 1
    fullyConnectedLayer(numResponses, 'name', 'fullconnect')
    regressionLayer('name', 'out')]; % Regression layer

%% Set parameters
% Specify training options, set the solver to 'adam'
options = trainingOptions('adam', ...
    'MaxEpochs', round(x(2)), ...
    'GradientThreshold', 1, ...
    'InitialLearnRate', x(3), ...
    'LearnRateSchedule', 'piecewise', ...
    'LearnRateDropPeriod', 800, ...
    'LearnRateDropFactor', 0.8, ...
    'MiniBatchSize', 240, ...
    'Verbose', 1, ...
    'Plots', 'none'); % Turn off training plots

%% Train BiLSTM
net = trainNetwork(P_train, tn_train', layers, options);

%% Training set predictions
train_simu = predict(net, P_train);
train_simu = mapminmax('reverse', train_simu', ts);

%% Test set predictions
test_simu = predict(net, P_test);
test_simu = mapminmax('reverse', test_simu', ts);

% Calculate fitness using root mean square error
fitness = sqrt(mean((test_simu - t_test).^2));
% fitness = sqrt(mean((test_simu - output_test).^2));

end
```

**%% 'func' in previous program ('Bi-LSTM-WO')**

```
%% Initialization
% This function initializes the first population of search agents
function Positions = initialization(SearchAgents_no, dim, ub, lb)

Boundary_no = size(ub, 2); % Number of boundaries (size of the second dimension)

% If the boundaries of all variables are equal and the user enters a single
% number for both ub and lb
if Boundary_no == 1
    Positions = rand(SearchAgents_no, dim).*(ub - lb) + lb;
end

% If each variable has a different lb and ub
if Boundary_no > 1
    for i = 1:dim
        ub_i = ub(i);
        lb_i = lb(i);
        Positions(:, i) = rand(SearchAgents_no, 1).*(ub_i - lb_i) + lb_i;
    end
end
```

**%% Evaluation index calculation**

```
function [mae,mse,rmse,mape,error,errorPercent]=compute_error(x1,x2)
%This function is used to calculate the predicted and actual value of each error indicator
%    mae£ºMean absolute error
%    mse£ºMean Square Error
%    rmse£ºRoot mean square error
%    mape£ºMean absolute percentage error
%    error£ºAbsolute error
%    errorPercent£ºRelative Error
if nargin==2
    if size(x1,2)==1
        x1=x1';    %Converting column vectors to row vectors
    end

    if size(x2,2)==1
        x2=x2';    %Converting column vectors to row vectors
    end

    num=size(x1,2);%Total number of statistical samples
    error=x2-x1;    %Calculate the absolute error
    errorPercent=abs(error)./x1; %Calculate the absolute percentage error for each sample
```

```
        mae=sum(abs(error))/num; %Calculate the mean absolute error
        mse=sum(error.*error)/num;    %Calculate the mean square error
        rmse=sqrt(mse);          %Calculate the root mean square error
        cvrmse=rmse/mean(x2) %Calculate CV-RMSE
        mape=mean(errorPercent);    %Calculate the mean absolute percentage error

        %Results
        disp(['mae is£º    ',num2str(mae)])
        disp(['mse is£º    ',num2str(mse)])
        disp(['rmse is£º ',num2str(rmse)])
        disp(['cvrmse is£º ',num2str(cvrmse)])
        disp(['mape is£º ',num2str(mape*100),' %'])

    else
        disp('There is an error in the function call method, please check the number of input parameters')
    end
    end
```

## Highlights

1. A novel building plug-load electricity consumption prediction system was proposed.
2. The definition and classification of building plug loads were proposed.
3. The enhanced input system based on occupant behavior probability was proposed.
4. The optimized algorithms based on the Bi module and WO module were verified.
5. The optimal combination of input system and training algorithms was proposed.

**Declaration of interests**

☒ The authors declare that they have no known competing financial interests or personal relationships that could have appeared to influence the work reported in this paper.

☐The authors declare the following financial interests/personal relationships which may be considered as potential competing interests:

| |
|---|
| None |